Stochastic Structural Stability Theory applied to roll/streak formation in boundary layer shear flow

Brian F. Farrell*
Department of Earth and Planetary Sciences, Harvard University
24 Oxford Street, Cambridge, MA 02138, U.S.A.

Petros J. Ioannou†
Department of Physics, University of Athens
Panepistimiopolis, Zografos 15784, Greece
(Dated: November 8, 2010)

Stochastic Structural Stability Theory (SSST) provides an autonomous, deterministic, nonlinear dynamical system for evolving the statistical mean state of a turbulent system. In this work SSST is applied to the problem of understanding the formation of the roll/streak structures that arise from free-stream turbulence (FST) and are associated with bypass transition in boundary layers. Roll structures in the cross-stream/spanwise plane and associated streamwise streaks are shown to arise as a linear instability of interaction between the FST and the mean flow. In this interaction incoherent Reynolds stresses arising from FST are organized by perturbation streamwise streaks to coherently force perturbation rolls giving rise to an amplification of the streamwise streak perturbation and through this feedback to an instability of the combined roll/streak/turbulence complex. The dominant turbulent perturbation structures involved in supporting the roll/streak/turbulence complex instability are non-normal optimal perturbations with the form of oblique waves. The cooperative linear instability giving rise to the roll/streak structure arises at a bifurcation in the parameter of STM excitation parameter. This structural instability eventually equilibrates nonlinearly at finite amplitude and although the resulting statistical equilibrium streamwise streaks are inflectional the associated flows are stable. Formation and equilibration of the roll/streak structure by this mechanism can be traced to the non-normality which underlies interaction between perturbations and mean flows in modally stable systems.

I. INTRODUCTION

The physical mechanism of turbulence in shear flows is not yet comprehensively understood despite many recent advances in experiment, simulation and theory. The problem of shear flow turbulence can be divided into two components: transition from the laminar to the turbulent state and maintenance of the turbulent state. The transition problem results from the lack of an inflection in the velocity profiles of most boundary layer flows. Inflections are associated by the Rayleigh theorem with existence of robust instabilities that continue in viscous flows from the inflectional instability of the same velocity profile in an inviscid flow. The problem of observed robust disturbance growth in perturbation stable shear flows was solved when it was recognized that the non-normality of the underlying linear dynamics of shear flows allows perturbation growth in the absence of exponential instability. The concept of transient growth in shear flow has roots in the classical work of Kelvin and Orr [1, 2] who used analytical solutions of perturbation dynamics in idealized shear flows to provide example solutions demonstrating transient growth. This early work remained obscure presumably due to lack of a convincing physical application. Transient growth concepts were first applied in the modern context of linear operator non-normality to understanding the three dimensional baroclinic turbulence in the midlatitude atmospheric jet after comprehensive data collected beginning in the middle of the last century for the purpose of weather forecast provided convincing evidence that turbulence in the midlatitude jet stream was maintained by growth processes unrelated to exponential instability [3–5]. In the context of laboratory shear flows although three dimensional perturbations in the form of a roll/streak structure were observed in boundary layers (Townsend, 1956; Kline et al., 1967; Blackwelder and Eckelmann, 1979; Robinson, 1991) and related to the nonmodal lift-up growth mechanism [6] similarly comprehensive observational evidence for the mechanism of nonmodal growth in boundary layer flows awaited the advent of direct numerical simulation (DNS) at Reynolds numbers O(1000), for which turbulence is maintained in shear flow, and particle image velocimetry (PIV) of turbulent laboratory shear flows. The methods of non-normal operator analysis and optimal perturbation theory were first applied in the

*Electronic address: farrell@seas.harvard.edu
†Electronic address: pjioannou@phys.uoa.gr

context of laboratory shear flows to two dimensional disturbances [7]. It was believed at the time that secondary instability of finite amplitude two dimensional equilibria were the mechanism of transition [8, 9] and it was shown that these unstable two dimensional nonlinear finite amplitude equilibria could be readily excited by even very small optimal initial perturbations[10]. However, it became increasingly apparent from observation and simulation that the finite amplitude structures associated with transition are three dimensional and analysis of three dimensional optimal perturbation growth followed [11–17]. These analyses revealed that the optimally growing three dimensional structure is associated with cross-stream/spanwise rolls and associated streamwise streaks and is related to the linear lift up mechanism. The remarkable convected coordinate solutions for perturbation growth in unbounded shear flow [1] allow closed form solution for the scale independent structures producing optimal growth in three dimensional shear flow [13, 14]. These closed form optimal solutions in unbounded shear flow confirm the result found numerically in bounded shear flows that for sufficiently long optimizing times streamwise rolls produce optimal energy growth while for short optimizing times the optimal perturbations are oblique wave structures that synergistically exploit both the two dimensional shear and the three dimensional lift up mechanisms producing vortex cores oriented at an angle of approximately 60 degrees from the spanwise direction. And indeed, the roll/streak and oblique accompanying structure complex that is predicted to produce optimal growth by analysis of non-normal perturbation dynamics of shear flows has been convincingly seen in both observations and simulations [18–21] and shown to be essentially related to the non-normality of shear flow dynamics [22, 23].

Although the mechanism of non-normal growth has been clarified, and its importance in bypass transition and maintenance of the turbulent state is widely if not universally accepted, the route by which non-normality leads to formation of the roll/streak structure and the part played by this coherent structure, its nonlinear equilibration and its stability, in the transition to turbulence and maintenance of the turbulent state remains to be determined.

The most direct mechanism exploiting non-normality to form roll/streak structures is introduction of an optimal perturbation into the flow, perhaps by using a trip or other device [11, 15, 16]. A related approach is to stochastically force the flow, with stochastic forcing regarded as modeling surface roughness or free stream turbulence (FST). This mechanism can be analyzed using stochastic turbulence modeling (STM) [24–31]. Because of the non-normal nature of perturbation growth in shear flow, stochastic turbulence models are closely related to optimal perturbation dynamics. In conventional stochastic turbulence models the roll/streak structure is envisioned to arise from chance occurrence of optimal or near optimal perturbations in the stochastic forcing[29, 32–34]. These mechanisms exploit the linear non-normal growth process directly. However, the ubiquity of streak formation suggests, as argued by Shoppa and Hussein [19], that some form of instability process underlies the formation of streaks, that this instability involves an intrinsic association between the roll/streak structure and associated oblique waves and vortices, and that this three dimensional instability must differ qualitatively from the familiar laminar shear flow instability. Indeed, from a comparison of experiment with simulation Anderson et al. [35] conclude that the evidence "..corresponds to some fundamental mode triggered in the flat-plate boundary layer when subjected to high enough levels of free-stream turbulence..". Previously proposed exponential instability mechanisms include centrifugal instability [36] and the Craik-Leibovich instability [37]. Proposed algebraic growth mechanisms involve a streamwise average torque produced by interaction of discrete oblique waves[38, 39].

All these streak growth mechanisms rely on the dominant non-normal process in shear flow which is lift up of mean streamwise velocity by perturbation cross-stream velocity, while differing in the manner in which this cross-stream velocity arises.

The cross-stream/spanwise roll structure provides a powerful mechanism for forming streamwise streaks in shear flows whether episodically forced by an initial condition or continuously forced by an oblique wave structure. However, in the absence of feedback from the streak back to the roll this powerful streak formation mechanism does not result in instability although because of the large streak growth produced by a cross-stream/spanwise roll perturbation, placing even a very weak coupling of the streak to the roll, such as by a small spanwise frame rotation, results in destabilization [40, 41]. Turbulent Reynolds stress provides an alternative mechanism for producing the feedback between the streak and roll needed to destabilize the roll/streak structure. Indeed, if we observe a turbulent shear flow in the cross-stream/spanwise plane at a fixed streamwise location we see that at any instant there is a substantial torque from Reynolds stress divergence forcing cross-stream/spanwise rolls. The problem is that this torque is not systematic and so it vanishes in temporal or streamwise average. However, in the presence of a perturbation streak the symmetry in the spanwise direction is broken and the torque from Reynolds stress divergence can become organized to produce the positive feedback between the streak and roll required to destabilize this structure by continuously and coherently exploiting the powerful non-normal roll/streak amplification mechanism. The existence of this mechanism for destabilizing the roll/streak structure in turbulence makes it likely that some dynamical perturbation complex exists to exploit it. In this work we prove by construction that this is so by deriving a system of equations eigenanalysis of which reveals the unstable roll/streak/turbulence structure that is responsible for destabilizing turbulent shear flow to streak formation. This emergent instability can be understood as a synthesis of the streak formation mechanisms described above in which FST, rather than itself constituting the cross-stream velocity linearly forcing streak growth,

instead is organized by the perturbation streak into oblique waves that quadratically force the cross-stream/spanwise roll by inducing a Reynolds stress torque linearly proportional to streak amplitude thereby producing an emergent exponential instability of the combined roll/streak/turbulence complex. As a boundary layer develops in the presence of FST this exponential instability of organization of the roll/streak complex is the first non-viscous instability to occur. We remark that this coupling in the highly non-normal boundary layer shear flow of the roll and streak components by turbulent stresses resulting in destabilization of the roll/streak structure is analogous to the coupling of the torroidal and poloidal components of the magnetic field by the turbulent α effect which destabilizes the induction equation in the magnetic dynamo problem[42].

The challenge is to find a method of stability analysis analogous to the method of modes for laminar flow instability, but applicable to the emergent turbulence/mean flow interaction instability. Specifically, analysis of the cooperative instability of the roll/streak/turbulence complex requires constructing a dynamical system for evolving the consistent statistical mean of a turbulent state. What is required is a physically correct while at the same time a computationally accessible approximation to the evolution of the trajectory of the probability density function (pdf) of a turbulent system in phase space. We refer to this dynamical system as the stochastic structural stability theory (SSST) system. The approximate pdf of the turbulent state, which is carried forward in time by the SSST system dynamics, often evolves to a fixed point corresponding to a statistically steady turbulent state. This method for analyzing the dynamics of the pdf of a turbulent system was developed to study the phenomenon of spontaneous jet formation at global scale in planetary atmospheres [41, 43, 44] and has also been applied to the problem of spontaneous jet formation from drift wave turbulence in magnetic fusion devices[45]. In SSST the turbulence is simulated using a STM in which intrinsic excitation of perturbations by nonlinear scattering and extrinsic excitation by FST are parameterized as stochastic [46–49]. The STM provides an evolution equation for the quadratic statistics of the turbulent eddy field associated with a mean flow. In the STM the eddy field is expressed in terms of a covariance matrix from which the Gaussian probability density function approximation for the turbulence variance and quadratic fluxes can be obtained. Coupling a time dependent STM to an evolution equation for the streamwise mean roll/streak/shear complex produces a nonlinear dynamical system for the co-evolution of the roll/streak/shear and the self-consistent quadratic statistics of its associated turbulence: this is the SSST system.

The SSST equations incorporate a stochastic turbulence model but these equations are themselves deterministic and autonomous with dependent variables the streamwise mean roll/streak/shear complex and the streamwise mean covariance of the turbulence. The perspective on shear flow stability provided by these equations differs from the more familiar perspective based on perturbation stability of stationary laminar flows. In fact, the primary perturbation instability in SSST has no counterpart in the stability theory of laminar flow; it is rather a cooperative instability in which the evolving roll/streak/shear complex organizes the background turbulence covariance to produce flux divergences configured to amplify the roll/streak/shear complex leading to an emergent coupled roll/streak/shear plus turbulence instability that does not involve perturbation instability of the streak. The SSST equations approximate the nonlinear streamwise mean dynamics of the coupled roll/streak/shear plus turbulence complex and this system in many cases supports equilibration of the emergent roll/streak/shear complex and its consistent turbulence field at finite amplitude. Equilibrium between a mean flow and its associated field of turbulence requires that the momentum flux divergence arising from the turbulent and mean velocities produce a stationary state of balance with the streamwise mean flow forcing and dissipation. The remarkable fact is that the turbulence, which depends on the roll/streak/shear complex, and the roll/streak/shear complex, which depends on the turbulence, quite generally adjust to produce such balanced states.

While the solution trajectory of an initially unstable SSST state generally converges to a fixed point representing a state of balance among the mean flow forcing and advection, the turbulent Reynolds stress divergence, and the damping; these finite amplitude equilibria may lose structural stability as a function of the STM excitation parameter and this instability then leads either to another equilibrium or to a time dependent limit cycle or chaotic solution [41, 43, 44, 50, 51]. Chaotic trajectories of the SSST system correspond not to the familiar chaos of an individual turbulent state trajectory but rather to chaos of the ensemble mean turbulent state. An example of this kind of chaos is the irregular fluctuation of the mean flow/turbulence complex seen in drift wave turbulence [52].

In this work we concentrate on the emergence of roll/streak structures in boundary layers as an instability of interaction between FST and the streamwise mean flow and on the mechanism by which this instability equilibrates at finite amplitude to maintain a statistically stable mean roll/streak/turbulence structure. Stable roll/streak structures are initiated as an instability at a minimum intensity of FST and are maintained as statistically stationary structures over an interval of STM excitation parameter. The time dependent state initiated at higher levels of FST will be reported on elsewhere.

II. REVIEW OF STREAMWISE VORTEX FORCING BY OBLIQUE WAVES

The emergent SSST streak instability mechanism can be understood as a synthesis of mechanisms previously investigated in the study of streak formation in boundary layers and we begin by reviewing the mechanism of streamwise vortex forcing by oblique waves which has been used[38, 39, 53] to explain the streamwise mean vortex circulations observed by Klebanoff et al. [18]. These works ascribe streak formation to interaction of a specific mixture of Tollmien-Schlichting (TS) waves and oblique perturbations chosen to produce through quadratic advective interaction a zero streamwise wavenumber component. Consider a fluctuating eddy field and its associated Reynolds stresses $\overline{u_i u_j}$, where u_i is one of the three components of the eddy velocity field, u in the streamwise, x, direction; v in the cross-stream, y, direction; and w in the spanwise, z, direction. Here and in the sequel an overline denotes the streamwise average. Divergence of the Reynolds stress induces a streamwise mean force:

$$F_i = -\frac{\partial \rho \overline{u_i u_j}}{\partial x_j}.$$

The mean spanwise force is

$$F_z = -\frac{\partial \rho \overline{vw}}{\partial y} - \frac{\partial \rho \overline{w^2}}{\partial z}$$

and the mean cross-stream force is:

$$F_y = -\frac{\partial \rho \overline{vw}}{\partial z} - \frac{\partial \rho \overline{v^2}}{\partial y} \ .$$

Consequently the streamwise component of the mean torque $\vec{G} = \nabla \times \vec{F}$ is:

$$\begin{aligned} G_x &= \frac{\partial F_z}{\partial y} - \frac{\partial F_y}{\partial z} \\ &= \left(\frac{\partial^2}{\partial z^2} - \frac{\partial^2}{\partial y^2} \right) \rho \overline{vw} + \frac{\partial^2}{\partial y \partial z} \rho \left(\overline{v^2} - \overline{w^2} \right) \ . \end{aligned}$$

If the eddy field is spanwise homogeneous no streamwise mean torque is present. However, it is a remarkable fact that quite generally in three dimensional flows when spanwise symmetry is broken mean torques arise that maintain streamwise mean vortices.

As an example it is instructive to review the case of an unbounded domain with a flow field consisting of two oblique structures in the x, z plane with wave vector (k, m) inclined at an angle $\Theta = \pm \tan^{-1}(m/k)$ to the streamwise direction:

$$u = u_0 \cos mz e^{ikx+ily} \ , \ v = v_0 \sin mz e^{ikx+ily} \ , \ w = w_0 \cos mz e^{ikx+ily} \ , \tag{1}$$

With velocity components satisfying non-divergence:

$$iku_0 + ilv_0 + mw_0 = 0 \ .$$

The Reynolds stresses for this flow are:

$$\overline{vw} = \frac{1}{4} \Re(v_0 w_0^*) \sin 2mz \ , \ \overline{v^2} = \frac{1}{2} |v_0|^2 \cos^2 mz \ , \ \overline{w^2} = \frac{1}{2} |w_0|^2 \sin^2 mz \ .$$

The spanwise dependence of the Reynolds stresses implies a streamwise mean force $F_y(z)$ in the cross-stream plane inducing streamwise mean toque:

$$G_x = -\rho m^2 \Re(v_0 w_0^*) \sin 2mz \ .$$

Note that this torque has double the spanwise wavenumber of the perturbation field. There is no streamwise torque induced by a single oblique wave when $m = 0$. Perhaps less obvious is that no Reynolds stress torques are induced by streamwise rolls with $k = 0$ because continuity requires v_0 and w_0 be in quadrature and therefore $\Re(v_0 w_0^*) = 0$.

The vanishing of the torque in these two limiting cases is made clear by using the continuity equation to write

$$G_x = -\rho \frac{km^2}{l} \Re(u_0 w_0^*) \sin 2mz \ ,$$

it is also immediate from this expression that for given square wavenumber $k^2 + m^2$ the torque is maximized for oblique waves with $\Theta \equiv \tan^{-1}(m/k) = 54.7^0$.

For unbounded constant shear flow, $U = \alpha y$, plane wave solutions in closed form exist [1]. For such a flow it can be easily shown that the Reynolds stress for an initial eddy field in the form of the oblique perturbations in the form (1) is:

$$\overline{vw}(t) = \frac{1}{4} \frac{k^2 + l^2 + m^2 + l^2}{k^2 + m^2 + (l - \alpha k t)^2} e^{-g(t)} \Re(v_0 w_0^*) \sin 2mz \ ,$$

where $e^{-g(t)}$ is the decay due to dissipation. The time dependent Reynolds stress produced by an oblique wave in constant shear flow produces torque with constant spatial structure and as a result coherent mean streamwise torque over its lifecycle. Also it can be shown using this closed form solution [13] that energy growth over short time intervals is maximized for oblique perturbations with $\Theta = 63^0$ which is very close to the orientation of the oblique wave maximizing the induced torque. It is consistent then that near $\Theta = 63^0$ lies the oblique waves that producing the greatest mean streamwise torques when integrated over their life cycle.

However, the fact that a specific pair of plane oblique waves force streamwise vortices does not explain the presence of streamwise vortices when the mean flow and the perturbation field statistics are spanwise uniform. Remarkably, while no mean streamwise torque arises from turbulence in a fluid with only a constant shear in the cross-stream direction, the slightest spanwise structure in the streamwise flow induces coherent streamwise mean torques. An example of this phenomenon obtained by imposing the mean streamwise perturbation test function $\delta U = \epsilon \cos(\pi y/(2L_y)) \cos(2\pi z/L_z)$ on a Couette flow is shown in Fig.1. This result was obtained using the STM described in section III by first calculating the equilibrium perturbation velocity covariance maintained by stochastic excitation in the perturbed streamwise mean flow and then obtaining from this perturbation velocity covariance the resulting Reynolds stress induced torque. This coherent torque arises because the eddy field is modified by the spanwise variation of the streamwise streak. This induced torque in turn modifies the mean flow which by interaction with the eddy field produces a modified torque. Most mean flow perturbations organize torques that do not exactly amplify that mean flow perturbation, as is the case for the perturbation in Fig. 1. However, exponential growth of streamwise mean flows and associated eddy fields would result, at least for sufficiently small perturbations, if the mean flow perturbation were to organize precisely the eddy field required for its amplification. We show constructively below that these cooperative instability structures arise quite generally by using an eigenanalysis to solve for them. Boundary layer flows in general support this structural instability in the presence of sufficient FST. For a range of FST intensities this structural instability equilibrates at finite amplitude producing stable but strongly inflected spanwise streaks.

III. FORMULATION OF THE COMPOSITE ROLL/STREAK/TURBULENCE DYNAMICS

We decompose the velocity fields into streamwise mean components (indicated uppercase) and perturbations (indicated lowercase) so that the total streamwise velocity in the x direction is $U(y,z,t) + u(x,y,z,t)$, the cross-stream velocity in the y direction is $V(y,z,t) + v(x,y,z,t)$, and the spanwise velocity in the z direction is $W(y,z,t) + w(x,y,z,t)$. The flow is confined to the channel $|y| \leq 1$, $|z| \leq L_z/2$ and the Reynolds number, R, is based on the half cross-stream channel distance $L_y = 1$. With constant velocity channel walls forcing a Couette flow as a laminar equilibrium the boundary conditions are $U(\pm 1, z, t) = \pm 1$, $V(\pm 1, z, t) = W(\pm 1, z, t) = 0$ and $u(x, \pm 1, z, t) = v(x, \pm 1, z, t) = w(x, \pm 1, z, t) = 0$ which imply that the normal vorticity $\eta = \partial_z u - \partial_x w$ satisfies the boundary condition $\eta(x, \pm 1, z, t) = 0$ and from continuity, $v_y(x, \pm 1, z, t) = 0$. Periodic boundary conditions are imposed in the spanwise direction.

We write perturbation equations about the streamwise mean flow, $U(z,y,t)$, neglecting the small spanwise and cross-stream mean flows, as it can be verified that $||V||, ||W|| << ||U||$. With this simplification the perturbation equations can be reduced, following steps similar to those used in the derivation of the Orr-Sommerfeld and Squire system [17, 54] , to two equations in the normal velocity, v, and normal vorticity, η. The resulting equations for the perturbations in these variables are:

$$v_t + \Delta^{-1} \left(U \Delta_x + U_{zz} v_x + 2U_z v_{xz} - U_{yy} v_x - 2U_z w_{xy} - 2U_{yz} w_x - \Delta \Delta v / R \right) = F_v \ , \tag{2a}$$

$$\eta_t + U \eta_x - U_z v_y + U_{yz} v + U_y v_z + U_{zz} w - \Delta \eta / R = F_\eta \ . \tag{2b}$$

where Δ^{-1} is the inverse of the Laplacian, $\Delta \equiv \partial^2_{xx} + \partial^2_{yy} + \partial^2_{zz}$. On the RHS F_v and F_η represent deviations of the perturbation-perturbation advection from its streamwise average, as is the convention in Reynolds averaging, together with input from FST. A parameterization of these terms will be specified in the next section.

The spanwise and streamwise velocity expressed in terms of the variables v and η are:

$$\Delta_h w = -v_{yz} - \eta_x \quad , \quad \Delta_h u = -v_{yx} + \eta_z, \tag{3}$$

in which $\Delta_h \equiv \partial^2_{xx} + \partial^2_{zz}$ denotes the horizontal Laplacian.

The mean streamwise flow, U, evolves according to

$$U_t = -(UV + \overline{uv})_y - (UW + \overline{uw})_z + \Delta U/R \ . \tag{4}$$

The mean streamwise flow U is maintained against dissipation by the streamwise component of the force from the eddy Reynolds stresses and by the acceleration induced by the mean roll circulation $-(UV)_y - (UW)_z$ which can be written equivalently as $-U_y V - U_z W$. In spanwise independent flows this term reduces to $-U_y V$ and represents the familiar lift up mechanism [6]. In order to evolve the streamwise mean flow the eddy Reynolds stresses and the fields V and W associated with the roll circulation are required. We define the streak perturbation as the component of U that deviates from its spanwise average, $[U] = \int_0^{L_z} U dz/L_z$, so that that the velocity associated with the streak is $U_s = U - [U]$.

The streamwise mean cross-stream and spanwise velocities; V and W respectively, can be obtained from the mean streamfunction $\Psi(y, z, t)$:

$$V = -\Psi_z \quad , \quad W = \Psi_y \ , \tag{5}$$

which evolves according to the equation for mean streamwise vorticity $\Delta\Psi$.

$$\Delta\Psi_t = (VW + \overline{vw})_{zz} - (VW + \overline{vw})_{yy} - (W^2 - V^2 + \overline{w^2} - \overline{v^2})_{yz} + \Delta\Delta\Psi/R \ . \tag{6}$$

This vortex is forced by the torque arising from perturbation Reynolds stresses as discussed in the previous section. The eddy torque is the only forcing maintaining the roll circulation against dissipation as the mean terms in (6) produce only advection of streamwise vorticity in the cross-stream/spanwise plane.

Equations (2a, 2b, 4, 6) comprise the roll/streak/turbulence dynamics. In the absence of FST this system has as a stable equilibrium solution only the perturbation stable Couette flow $U = y$, $V = W = 0$. In the presence of FST the combined roll/streak/turbulence dynamics includes the ensemble mean Reynolds stress from the perturbation field described by (2a, 2b, 4, 6) giving rise to new equilibria. We next show how SSST can be used to find these new stable equilibria.

IV. THE SSST SYSTEM GOVERNING ROLL/STREAK/PERTURBATION DYNAMICS

The SSST system[43] includes the three components of the streamwise mean flow (4, 6), and the ensemble mean Reynolds stress from the perturbations (2a, 2b). In the perturbation equations (2a, 2b) stochastic excitation is introduced to parameterize both the exogenous FST and the endogenous scattering by eddy-eddy interactions. The perturbation equations with this parameterization comprise the Stochastic Turbulence Model (STM). The STM provides accurate eddy structure at the energetic scales because the highly non-normal dynamics associated with the non-normal linear operator in strongly sheared flows predominates in determining the perturbation structure [28, 55]. This parameterization has been widely used to describe the dynamics of turbulence in channel flows [24, 26, 27, 29–33] and has also been instrumental in advancing robust control of channel flow turbulence [28, 56–59]. The STM has also been verified to determine with great accuracy the eddy structure of the midlatitude atmosphere [48, 49, 60–64].

We use Fourier expansion in the streamwise direction, x, for the perturbations that deviate from the streamwise mean:

$$v = \sum_k \hat{v}_k(y, z, t) e^{ikx} \ , \ \eta = \sum_k \hat{\eta}_k(y, z, t) e^{ikx} \ , \tag{7}$$

in which the $k = 0$ streamwise wavenumber is excluded. We discretize the perturbation equations (2a, 2b) in the cross-stream, y, and spanwise, z, directions with the state $\hat{\phi}_k = [\hat{v}_k, \hat{\eta}_k]^T$ prescribed by the normal velocity and vorticity on a $y - z$ grid for each x Fourier component. Streamwise mean Reynolds stresses can be obtained from the streamwise mean covariance matrix of the perturbation state. Under the ergodic assumption this streamwise mean covariance is the same as the ensemble mean covariance[89], $\mathbf{C}_k = < \hat{\phi}_k \hat{\phi}_k^\dagger >$ (in this expression $< \cdot >$ denotes ensemble averaging

and the subscript indicates that the statistics are those of the eddy field components with streamwise wavenumber k).

In order to evolve the perturbation covariance we must first specify an excitation to maintain the FST. We take an excitation in (2a, 2b) that is delta correlated in time and of the general form:

$$\begin{pmatrix} F_v \\ F_\eta \end{pmatrix} = \mathbf{F}\xi$$

where $\xi(t)$ is a normally distributed independent random column vectors of length equal to twice the number of discretization points, that satisfies:

$$< \xi_i(t)\xi_j(s) >= \delta_{ij}\delta(t-s),$$

with the structure matrix $\mathbf{F}$ determining the spatial coherence of the forcing of the cross-stream velocity and vorticity i.e. the fluid is excited delta correlated in time with a spatial structure that is a superposition of the columns of $\mathbf{F}$. In the ensemble equations for the quadratic eddy covariance at streamwise wavenumber k the stochastic forcing enters through its covariance $\mathbf{Q}_k$:

$$\mathbf{Q}_k = \mathbf{F}\mathbf{F}^\dagger \ . \tag{8}$$

The qualitative features of the SSST dynamics are insensitive to the structure of the forcing, $\mathbf{Q}_k$, as long as it excites the most energetic structures. The reason is the high non-normality of the perturbation operator which leads to strong amplification of a few optimal structures that in turn determine the perturbation field[24, 26].

We take $\mathbf{Q}_k$ to be proportional to $\mathbf{M}_k^{-1}$, where $\mathbf{M}_k$ is the metric that determines the perturbation kinetic energy at streamwise wavenumber k through the inner product:

$$E_k = \hat{\phi}_k^\dagger \mathbf{M}_k \hat{\phi}_k \ . \tag{9}$$

This forcing covariance excites the system so that each degree of freedom receives equal energy. The energy metric is given by

$$\mathbf{M}_k = \frac{1}{4}\left(\mathbf{L}_u^{k\dagger}\mathbf{L}_u^k + \mathbf{L}_v^{k\dagger}\mathbf{L}_v^k + \mathbf{L}_w^{k\dagger}\mathbf{L}_w^k\right) \ , \tag{10}$$

where $\hat{u}_k = \mathbf{L}_u^k\hat{\phi}_k$, $\hat{v}_k = \mathbf{L}_v^k\hat{\phi}_k$, and $\hat{w}_k = \mathbf{L}_w^k\hat{\phi}_k$. Explicitly, the linear operator $\mathbf{L}_v^k$ is the projection,

$$\mathbf{L}_v^k = [\mathbf{I} \ \ \mathbf{0}] \ , \tag{11}$$

while the two other linear operators are obtained using Equation (3):

$$\mathbf{L}_u^k = \begin{pmatrix} -ik\Delta_h^{-1}\partial_y & 0 \\ 0 & -\Delta_h^{-1}\partial_z \end{pmatrix} \ , \ \mathbf{L}_w^k = \begin{pmatrix} -\Delta_h^{-1}\partial_{yz}^2 & 0 \\ 0 & -ik\Delta_h^{-1} \end{pmatrix} \ . \tag{12}$$

The ensemble averaged covariance evolves according to the deterministic Lyapunov equation [47]:

$$\frac{d\mathbf{C}_k}{dt} \ = \ \mathbf{A}_k(U)\mathbf{C}_k \ + \mathbf{C}_k\mathbf{A}_k^\dagger(U) \ + \ f^2\mathbf{Q}_k \ , \tag{13}$$

in which f^2 is an amplitude factor and $\mathbf{A}_k(U)$ is the linear operator in (2a, 2b) which depends on the streamwise flow $U(y,z,t)$. In matrix form the operator $\mathbf{A}_k$ in (13) is:

$$\mathbf{A}_k(U) \ = \ \begin{pmatrix} \mathbf{L}_{OS} & \mathbf{L}_{C_1} \\ \mathbf{L}_{C_2} & \mathbf{L}_{SQ} \end{pmatrix} \ , \tag{14}$$

with

$$\mathbf{L}_{OS} = \Delta^{-1}\left(-ikU\Delta + ik(U_{yy} - U_{zz}) - 2ikU_z\partial_z - 2ik(U_z\partial_{yyz}^3 + U_{yz}\partial_{yz}^2)\Delta_h^{-1} + \Delta^2/R\right), \tag{15a}$$

$$\mathbf{L}_{C_1} = 2k^2\Delta^{-1}\left(U_z\partial_y + U_{yz}\right)\Delta_h^{-1}, \tag{15b}$$

$$\mathbf{L}_{C_2} = U_z\partial_y - U_y\partial_z - U_{yz} + U_{zz}\partial_{yz}^2\Delta_h^{-1}, \tag{15c}$$

$$\mathbf{L}_{SQ} = -ikU\Delta + ikU_{zz}\Delta_h^{-1} + \Delta/R \tag{15d}$$

The covariances, $\mathbf{C}_k$, evolved by (13) provides the Reynolds stresses for the mean flow equations (4, 6). For example the Reynolds stress $\overline{uv}$ is given by:

$$\overline{uv} = \frac{1}{2}\mathrm{Re}\left(\mathrm{diag}\left(\sum_{i=1}^{n}\mathbf{L}_u^{k_i}\mathbf{C}_{k_i}\mathbf{L}_v^{k_i\dagger}\right)\right) \tag{16}$$

where diag denotes the matrix diagonal and n the number of streamwise harrmonics. All the Reynolds stresses can be written similarly as linear functions of the covariance matrix and the streamwise mean equations (4, 6) can then be expressed concisely in the form:

$$\frac{d\Gamma}{dt} = G(\Gamma) + \mathbf{L}\mathbf{C} \tag{17}$$

where $\Gamma \equiv [U, \Psi]^T$ denotes the streamwise mean flow, G a function of the mean flow that includes the dissipation and external forcing, $\mathbf{C} = [\mathbf{C}_{k_1}, \cdots, \mathbf{C}_{k_n}]$ and $\mathbf{L}\mathbf{C}$ is the forcing of the mean by the Reynolds stresses, with $\mathbf{L}$ a linear operator.

Equations [(13), (17)] comprise the SSST system for the roll/streak/turbulence dynamics:

$$\frac{d\mathbf{C}_k}{dt} = \mathbf{A}_k(\mathbf{P}\Gamma)\mathbf{C}_k + \mathbf{C}_k\mathbf{A}_k^\dagger(\mathbf{P}\Gamma) + f^2\mathbf{Q}_k\ , \tag{18a}$$

$$\frac{d\Gamma}{dt} = G(\Gamma) + \mathbf{L}\mathbf{C}\ , \tag{18b}$$

with $\mathbf{P}$ the projection of Γ onto the mean streamwise flow so that $\mathbf{P}\Gamma = U$. The SSST dynamics can be written concisely as

$$\frac{d\chi}{dt} = S(\chi)\ , \tag{19}$$

by defining the SSST state $\chi = [\mathbf{C}, \Gamma]^T$. The equilibrium states satisfy $S(\chi_{eq}) = 0$.

Equation (19) constitutes a closed, deterministic, autonomous, nonlinear system for the co-evolution of the streamwise mean flow and its consistent field of turbulent eddies. Although the effects of the turbulent fluxes are retained in this system, the fluctuations associated with turbulent eddy dynamics are suppressed so that the dynamics of turbulent eddy/mean flow interaction and particularly the equilibria arising from this interaction are revealed with clarity. These nonlinear equilibrium states are intrinsically associated with the turbulence and are therefore dynamically distinct from coherent nonlinear states that have been extensively studied in geophysical [66, 67] and in laboratory shear flows[68–70].

The SSST system is globally stable [43] and the attractor of the SSST system may be a fixed point, a limit cycle, or a chaotic attractor. Examples of each of these behaviors has been found in the SSST description of geophysical and plasma turbulence[41, 43, 45].

The concept of the SSST system trajectory is novel because it is not the trajectory of a realization of the turbulent system but rather the trajectory of the statistical mean state of the turbulence which evolves on the time scale of the mean flow.

The SSST system introduces a new stability concept to fluid dynamics which is the stability of an equilibrium between a mean flow and its consistent field of turbulence. This stability theory generalizes the traditional hydrodynamic stability theory of Rayleigh[71]. If a mean flow is perturbation unstable (in the sense of Rayleigh) it is also structurally unstable (in the sense of SSST). However, the converse is not true and perturbation stability does not imply structural stability. In fact, emergence of roll/streak structures in shear flow will be shown to occur in association with structural instability of a perturbation stable state.

V. STABILITY ANALYSIS OF ROLL/ STREAK/ TURBULENCE EQUILIBRIA

Assume that for the given forcing covariance, $f^2\mathbf{Q}_k$, the equilibrium $\chi_{eq} = [\mathbf{C}_{eq}, \Gamma_{eq}]^T$ of the SSST equations (18) has been determined. We can study its stability by linearizing the SSST system about this equilibrium. The perturbation equations take the form

$$\frac{d\delta\mathbf{C}_k}{dt} = \mathbf{A}_k(\mathbf{P}\Gamma_{eq})\delta\mathbf{C}_k + \delta\mathbf{C}_k\mathbf{A}_k^\dagger(\mathbf{P}\Gamma_{eq}) + \delta\mathbf{A}_k\mathbf{C}_{keq} + \mathbf{C}_{keq}\delta\mathbf{A}_k^\dagger\ , \tag{20a}$$

$$\frac{d\delta\Gamma}{dt} = \left.\frac{\partial G}{\partial\Gamma}\right|_{\Gamma_{eq}}\delta\Gamma + \mathbf{L}\delta\mathbf{C}\ . \tag{20b}$$

where $\delta\Gamma = [\delta U, \delta\Psi]^T$ is the perturbation in the mean flow quantities: the streamwise flow, δU, and the roll streamfunction, $\delta\Psi$. The perturbation to the operator, $\mathbf{A}_k$, that controls the eddy field is $\delta\mathbf{A}_k$. This operator perturbation is produced by perturbation to the mean streamwise flow, δU. Setting $\delta\chi \equiv [\delta\mathbf{C}, \delta\Gamma]^T$ the perturbation equations can be written concisely as:

$$\frac{d\delta\chi}{dt} = \mathcal{L}\delta\chi \tag{21}$$

The linear operator $\mathcal{L} \equiv \partial S/\partial\chi|_{\chi_{eq}}$ depends on the equilibrium state $\chi_{eq} = [\mathbf{C}_{eq}, \Gamma_{eq}]^T$ which in turn depends on the Reynolds number R, the channel geometry, the mean flow forcing, and the stochastic excitation $f^2\mathbf{Q}_k$. Eigenanalysis of the linear operator $\mathcal{L}$ then determines the structural stability of this equilibrium roll/streak/turbulence complex[90].

The familiar laminar Couette flow equilibrium $\Gamma_{eq} = [U_{eq} = y,\ \Psi_{eq} = 0]^T$ and $\mathbf{C}_{eq} = 0$ is a solution of the SSST equations (18) in the absence of FST ($f = 0$). Because at zero forcing the eddy covariance vanishes, $\mathbf{C}_{eq} = 0$, the first of the perturbation SSST equations (20) reduces to an unforced Lyapunov equation which inherits the perturbation stability of Couette flow at all Reynolds numbers[73], i.e. the stability of $\mathbf{A}(\mathbf{P}\Gamma_{eq})$. The second equation is asymptotically unforced and clearly stable so in the absence of FST the system (20) is structurally stable as well as perturbation stable. From this argument it is clear that structural instability of a flow that is perturbation stable in the sense of Rayleigh requires non-vanishing $\mathbf{C}_{eq}$ or equivalently non zero values of f.

In the presence of spanwise homogeneous FST there is a class of spanwise independent equilibria $\Gamma_{eq} = [U_{eq}(y), \Psi_{eq} = 0]^T$ with non vanishing $\mathbf{C}_{eq}$. In these equilibria the mean streamwise flow $U_{eq}(y)$ is maintained by a balance between diffusion and the component of Reynolds stress divergence $-(\overline{uv})_y$ in the inhomogeneous (cross-stream) direction. The equilibria are possible because all the Reynolds stresses are independent of z, and symmetry requires that $\overline{vw} = 0$. These spanwise independent ensemble equilibria in the presence of FST correspond to boundary layer flow equilibria that depart from the Couette profile in y but have no z dependence. We will demonstrate that for sufficient amplitude of FST these equilibria, while remaining perturbation stable, become structurally unstable giving rise to roll circulations with associated streaks.

For convenience the amplitude of the forcing, $\mathbf{Q}_k$, is chosen to maintain RMS perturbation velocity 1% of the mean Couette flow velocity when it is used to excite the Couette flow so that when this excitation is introduced into the perturbation variance equation as $f^2\mathbf{Q}_k$ the adjustable amplitude, f, corresponds approximately to RMS FST as a percentage of the mean flow velocity. RMS perturbation velocity is very nearly linearly proportional to f as f increases prior to the bifurcation to roll /streak equilibria although deviating slightly because the mean flow profile deviates from Couette as FST increases (cf. Fig. 6).

We demonstrate the structural instability of the spanwise independent equilibria $\Gamma_{eq} = [U_{eq}(y), \Psi_{eq} = 0]^T$ in the presence of FST concentrated in a single wavenumber k. This simple case reveals the character of the instability and the results do not change qualitatively when multiple wavenumbers of FST are included. We first examine an example at $R = 400$, wavenumber $k = 1$, and spanwise periodic channels on the interval $3/20 < L_z/(2\pi) < 3/10$. These channels are narrower than the minimal channel of Hamilton, Kim and Waleffe[74] (herafter HKW) for which $L_z/(2\pi) = 6/10$. The calculations were performed with $N_y = 21$ and $N_z = 20$ points. Convergence was verified by repeating the calculations at higher resolutions.

We use the power method to find the structure and growth rate of the most unstable eigenmode of the $\mathcal{L}$ operator in (21) for the spanwise independent equilibrium flow $\Gamma_{eq} = [U_{eq}(y),\ \Psi_{eq} = 0]^T$. Contours of the growth rate of the most unstable eigenmode as a function of STM excitation parameter f and channel width L_z are shown in Fig. 2. The maximum growth rate of the $\mathcal{L}$ operator increases with f and for a critical intensity, $f_c(L_z)$, the spanwise independent flow becomes structurally unstable with eigenmodes in the form of exponentially growing roll/streak structures. The growth rate decreases with channel width at constant f and for sufficiently narrow channels $L_z/(2\pi) < 0.205$ the spanwise independent mean flow is structurally stable for all f and no roll/streak equilibrium is supported, in qualitative agreement with the findings of the minimal channel simulations of Jimenez and Moin[75].

For a channel with $L_z/(2\pi) = 0.3$ the spanwise independent equilibrium is structurally unstable for $f > f_c = 8.25$. The growth rate of the most unstable eigenfunction for this channel with STM excitation parameter $f = 12.8$ is $\lambda = 0.0166$. The structure of the most unstable eigenfunction is shown in Fig. 3. The eigenfunction comprises both a mean flow perturbation, $\delta\Gamma$, and an eddy covariance perturbation, $\delta\mathbf{C}$. The Reynolds stresses associated with $\delta\mathbf{C}$ produce accelerations and torques in exact agreement with the mean flow perturbation consistent with exponential growth. These structural instabilities typically equilibrate to finite amplitude roll/streak equilibria similar in structure to the most unstable eigenfunction, as seen in Fig. 4. The critical f_c at which structural instability occurs is a bifurcation point in a diagram of equilibria as a function of f, as shown in Fig. 5, 6.

We denote by E_r the mean kinetic energy of the roll, obtained by averaging $(V^2 + W^2)/2$ over the channel; by E_U the mean kinetic energy of the streamwise mean flow, obtained by averaging $U^2/2$; by E_s the mean kinetic energy of the streak, obtained by averaging $U_s^2/2$; and by E_p the mean kinetic energy of the eddies, obtained by averaging $(\overline{u^2} + \overline{v^2} + \overline{w^2})/2$. As f increases the STM excitation parameter rises and the increasing Reynolds stress induces

departure of the cross-stream flow from the pure Couette flow but for $f < 8.25$ the mean flow remains uniform in the spanwise direction and these spanwise independent equilibria are stable fixed points of the SSST system. The RMS velocity of the perturbation field $\sqrt{E_p/2}$ is shown as a function of f in Fig. 6. Note that as the spanwise uniform equilibria bifurcate to roll/streak equilibria for $f > f_c = 8.25$ the rate of increase of perturbation RMS velocity decreases as the turbulence is diverted to drive the roll/streak structure which, being lightly damped, reaches high equilibrium velocity. It is interesting that the RMS velocity remains approximately 10% of the background flow velocity until forcing excitation $f_u = 13.5$ at which point the roll/streak equilibrium undergoes a second structural instability. The roll/streak equilibria for $f_c < f < f_u$ are perturbation stable, and the breakdown that occurs at f_u is due to a secondary structural instability of the finite amplitude roll/streak. This secondary structural instability will be examined in future work.

We next demonstrate structural instability of the Couette flow in the minimal channel considered by HKW[74] taking $L_z/(2\pi) = 0.6$, $R = 400$ and the smallest streamwise wavenumber in the HKW channel, $k = 1.143$. These calculations were made with $N_y = 21$ and $N_z = 40$ points. This flow bifurcates from spanwise independent equilibria to spanwise dependent equilibria at $f_c = 5.82$ as shown in Fig. 7. Note the qualitative similarity with the bifurcation diagram for the smaller channel shown above. Both the RMS streak velocity and the RMS roll velocity vary as $\sqrt{f - f_c}$ near the the bifurcation point (dashed curve in Fig. 7) consistent with a supercritical pitchfork. At $f_u = 8.45$ the roll-streak equilibrium loses structural stability and no nearby equilibrium or periodic solution exists for $f > f_u$. For values close to this second structural instability the equilibria exhibit a $\sqrt{f_u - f}$ behavior consistent with a second order subcritical bifurcation which will be examined in future work. The most unstable perturbation of the SSST system about the unstable equilibrium state without roll/streak structure is shown for STM excitation parameter $f = 8.4 < f_u$ in Fig. 8.

VI. STRUCTURE OF THE ROLL/STREAK EQUILIBRIA

The streamwise mean flows of the structurally stable roll/streak equilibria in the HKW channel for STM excitation parameter in the interval $f_u > f > f_c$ are shown in Fig. 9. These equilibria exhibit streamwise high and low speed streaks that increase in amplitude as f increases. A useful measure of streak strength is its lift angle[23] which we define here as:

$$\theta_s = \max \tan^{-1} \left(\frac{\partial_z U}{\partial_y [U]} \right) ,$$

where $[U]$ is the spanwise average streamwise mean flow U. These equilibrium streaks reach $\theta_s = 56^o$ at $f = 8.45$. Despite their high lift angles all these equilibria are perturbation stable. The eigenvalues, σ, of the perturbation operators, $\mathbf{A}_k$, for the flows in Fig. 9 are shown in Fig. 10. Note the emergence of a mode with frequency $\sigma_i = 0$ as the streak increases in amplitude with increase in f. This is the sinuous mode that is associated with the spanwise inflection of the streak and that is often assumed to be responsible for streak breakdown[54, 74, 76–78] . However at $f = 8.45$ the roll/streak flow is still robustly stable and the instability that occurs at $f = 8.45$ is solely a structural instability of the cooperative turbulence/mean flow SSST dynamics.

Despite the large lift angle the equilibrium streamwise mean flows do not resemble the mean flows of the turbulent state. In Fig. 11 we compare the spanwise averaged streamwise mean flow $[U]$ for the flows with STM excitation parameter $f = (8.4,\ 7.5,\ 6)$ with the corresponding time averaged mean flow in the turbulent HKW channel. The equilibrium mean flows that occur in this range of STM excitation parameter indicate that these roll/streak equilibria are laminar. Indicative of this laminar regime is the viscous dissipation of the streamwise mean flow:

$$D = \frac{1}{R} \int_0^{L_z} dz \int_{-L_y}^{L_y} dy (U_y^2 + U_z^2 + V_y^2 + V_z^2 + W_y^2 + W_z^2) ,$$

The ratio D/D_C, where D_C is the dissipation associated with the Couette flow, of the equilibria for FST intensities $8.45 > f > f_c = 5.82$ is in the range $1 < D/D_C < 1.4$ while this ratio is of order 3 in the turbulent state.

The laminar roll/streak equilibria shown in Fig. 9 have spanwise wavenumber 2. The spanwise width of the channel is $90y^+$ for the equilibrium with $f = 8.4$ (the wall unit is defined as $y^+ \equiv 1/\sqrt{R[U_y]}$, where R is the Reynolds number and $[U_y]$ is the mean shear at the boundary) implying streak spacing $45y^+$ which is half that found in turbulent boundary layers. However, it should be kept in mind that this wall unit is being calculated for an essentially laminar flow. In section VIII we show that this spacing does agree with the observed streak spacing of 2 displacement thicknesses that is observed in laminar boundary layers before transition [79].

Consider the mechanism maintaining the roll/streak structure at STM excitation parameter $f = 8.4$ (Fig. 9d). The roll circulation is maintained against friction only by the turbulent stress divergence in (6) as the quadratic streamwise

mean terms in (6) do not generate mean streamwise vorticity. The cross-stream/spanwise acceleration $(\dot{V}, \dot{W})$ due to the eddy flux divergence is shown in Fig. 12c. Note that this acceleration is consistent with the circulation shown in Fig. 13a. The acceleration induced by the mean momentum flux divergence is subdominant in these equilibrium solutions and as a result the total acceleration $(\dot{V}, \dot{W})$ has the structure of the acceleration induced by the eddies as shown in Fig 13c and Fig 13a.

While the roll circulation is maintained against friction solely by the torque induced by the Reynolds stress divergences, the streak is influenced both by Reynolds stress divergence and by mean momentum flux divergence (cf. Eq. 4). The mean momentum flux divergence can be identified with the lift up mechanism as shown in Fig. 12b and this mechanism dominates in the streak maintenance (cf. Fig. 12b and Fig. 12d). The eddy Reynolds stress divergence, shown in Fig. 12d, tends to damp the streak consistent with the eddies extracting energy from the spanwise shear. This mean deceleration of the streak by the 3-D eddies in laboratory shear flow contrasts with the acceleration by quasi 2-D eddies that is primarily responsible for jet formation in planetary atmospheres[80–82]. In compensation for the loss of this dominant 2-D jet formation mechanism, these 3-D shear flows gain an indirect pathway for maintenance of the streak: the Reynolds stress divergences induce roll circulations which through the lift-up mechanism maintain the streaks against both viscous dissipation and the deceleration induced by the turbulent Reynolds stress divergence. This dual role of the eddy field in maintaining the equilibrium roll/streak structure will be discussed further in the next section.

We turn now to the structure of the eddy field at equilibrium. Eddy structures can be ordered in energy by eigenanalysis of $\mathbf{M}^{1/2}\mathbf{C}\mathbf{M}^{1/2}$, where $\mathbf{M}^{1/2}$ denotes the square root of the metric $\mathbf{M}$. Eigenfunctions of $\mathbf{M}^{1/2}\mathbf{C}\mathbf{M}^{1/2}$ in descending order of eigenvalue define the empirical orthogonal function (EOF) or Karhunen-Loeve decomposition of the eddy field. The percentage of the energy accounted for by each of the first 40 gravest modes of the covariance is shown in Fig. 14 for STM excitation parameter $f = 5$, for which the flow is spanwise uniform, and also for intensity parameters $f = 6,\ 7.5,\ 8.4$. It is clear that the variance is spread over many structures but as f increases the first EOF begins to dominate and its structure becomes a good representation of the eddy structure. This dominant EOF for the equilibrium structure at $f = 8.4$ is shown in Fig. 15. This eddy field is characterized by sinuous oblique waves centered at the wings of the streak and slanted in the vertical. This is the structure that produces the coherent torques maintaining the roll circulation. The dominant EOF is close in structure to the least stable mode of the flow which is shown in Fig. 16. Note however that this mode is robustly stable so it is maintained by excitation and non-normality, with the latter dominant. The large excitation of the mode is due to the interaction between this mode and the other modes of the system as revealed by its optimal excitation structure which is its adjoint[7, 47, 83]. The adjoint of the least stable mode in the energy inner product is shown in Fig. 17. An initial condition consisting of its adjoint excites the least stable mode at amplitude a factor 1900 greater than an initial condition consisting of the least stable mode itself so the mode arises out of the FST primarily due to excitation of its adjoint.

Because the excitation is chosen to be white in energy and all modes are stable the structure of the eddy field can be understood dynamically by examining optimal structure evolution. The optimal perturbation that leads to the greatest growth in energy in 10 time units for the equilibrium at $f = 8.4$ is shown in Fig. 18. The energy growth of this optimal is close to the energy growth of the adjoint of the least stable mode (cf. Fig. 19). Evolution of the maximum mean streamwise torque, G_x, induced by the Reynolds stress divergence of these optimal perturbations is also shown in Fig. 19. The torque increases as the perturbation energy increases. The energy evolution of the $t = 10$ optimal for the equilibria with $f = 7.5$ and $f = 5$, for which value the flow is spanwise independent, are also shown. The structure of the optimal when it reaches its maximum energy at $t = 15$ is shown in Fig. 20. The structure of this evolved optimal perturbation is similar to the structure of evolved optimals in equilibria at lower FST intensities as expected from the universality of the dynamics of oblique perturbations in three dimensional shear flows[1, 13, 14, 84]. The spanwise streak serves to collocate the perturbation structures aligning them so that the spanwise Reynolds stress divergence produce torques in phase with the evolving roll.

Finally we note that when the total field of the equilibrium mean flow and a typical realization of the eddy field are plotted together only a weak undulation of the streak structure can be discerned as is observed with laminar streaks before transition. For example a sample realization of the total equilibrium flow at STM excitation parameter $f = 8.4$ is shown in Fig. 21.

VII. MECHANISM OF ROLL/STREAK EQUILIBRATION

We wish to gain an understanding of the dynamics underlying equilibration of the structural instability of the spanwise independent flow in part to provide insight into turbulent equilibria in general and in part as a first step in understanding how loss of structural stability by these roll/streak equilibria at $f = 8.45$ leads to transition to to a time dependent state.

We will describe the equilibration of the structural instability of the spanwise independent flow at STM excitation

parameter $f = 8.4$ and in particular show how the inflectional mode is instrumental in producing the equilibrium. When the most unstable SSST eigenfunction is introduced into the spanwise independent flow, it grows exponentially at rate $\lambda = 0.014$ as predicted by SSST theory and finally equilibrates as can be seen in Fig. 22. As the STM excitation parameter approaches $f = 8.4$ oblique non-normal wave perturbations dominate the structures forcing the roll through their Reynolds stress and these produce a roll/streak equilibrium with highly inflected streaks (cf Fig. 9d). In association with this inflection the primary inflectional mode (with structure as in Fig. 16) approaches the stability boundary (cf Fig. 10d). Because it is drawing energy from the streak this mode produces strong downgradient Reynolds stresses that damp the mode while the Reynolds stress it produces to force the roll circulation are relatively weak. In order to compare the relative contribution of the direct downgradient Reynolds stress due to the inflectional mode in damping the streak with the mode's indirect Reynolds stress effect in forcing the roll circulation and thereby building the streak we artificially impose a modification of the real part of the eigenvalue of the mode at equilibrium, σ_{rE}, specifically we set the growth of this mode equal to $9/10\sigma_{rE}$ and $11/10\sigma_{rE}$, and integrated forward the SSST equations in order to determine the mean flow tendency. When the mode is less stable the perturbation energy increases, the associated roll circulation also increases as it is directly forced by the oblique structure of the perturbations, but the streak decreases because the enhanced downgradient fluxes by the less damped mode dominate over the increase in the streak induced by the roll circulation. The opposite happens when the mode is made more stable, as shown in Fig. 23.

We conclude that the primary mechanism of streak stabilization at high FST is the inflectional mode. As the f rises above $f = 8.45$ the inflectional mode is no longer able to stabilize the streak and a second structural instability ensues at $f_u = 8.45$ in which the oblique waves further accelerate the roll/streak complex. However, the streak remains perturbation stable until a very high amplitude is reached at which point the flow becomes time dependent and aperiodic so that the notion of an unstable temporal mode is no longer well defined. We will not examine this time dependent regime further in this work.

VIII. MECHANISM PRODUCING THE SPANWISE STREAK SPACING

A fully turbulent boundary layer, such as that approximated by the Reynolds-Tiederman profile, is maintained by the ensemble of eddies in the boundary layer. It is commonly observed in turbulent boundary layers that spanwise streak spacing is approximately 100 y^+ with wall unit $y^+ \equiv \sqrt{\nu/(\partial U/\partial y)}$ and $\partial U/\partial y$ being evaluated at the boundary. As the boundary layer is itself approximately 50 y^+ in wall normal extent this spacing is consistent with a roll of unit aspect ratio confined to the boundary layer[85, 86].

We have concentrated on the formation of streaks from FST in which the deviation of the mean boundary layer flow profile from the stationary Couette flow is small compared with that found in fully turbulent boundary layers. In order to study streak spacing in a numerically resolved example we maintain a Blasius profile stationary with an appropriate body force[79], subject it to a supercritical STM excitation parameter, and obtain the maximum growth rate of the structural instability as a function of spanwise wavenumber m of the unstable streak using the power method. Growth rate of the most unstable SSST roll/streak eigenmodes at STM excitation parameter $f = 10$ in a Blasius boundary layer at Reynolds number $R_x = 1.6 \times 10^5$ (based on the distance from the leading edge) are shown in Fig. 24. The maximum SSST instability occurs at the wavenumber corresponding to a spacing between low speed streaks of $\Delta z = 2.4\delta_1$ where $\delta_1 = 1.72\sqrt{\nu x/U}$ is the displacement thickness, consistent with unit roll aspect ratio. Although the implied selectivity is not very strong this result also agrees with observations[79]. The maximum is achieved by oblique waves with obliqueness parameter $\Theta = \tan^{-1} m/k$, close to the value 53^0 obtained from the simple argument of section I. This agreement shows that the basic dynamics are captured by the oblique plane wave solutions on an unbounded constant shear flow[1, 13, 14, 84]. These structures are scale independent and the streaks that are formed by the SSST instability share the universal character of these oblique perturbations.

IX. DISCUSSION

There are a number of points we wish to emphasize in connection with the above results:

1. Streaks can arise from a spontaneous cooperative exponential instability of the roll/streak/shear plus turbulence complex.

2. At finite amplitude the streaks of the roll/streak/shear plus turbulence instability complex typically form stable nonlinear equilibria.

3. The cross-stream/spanwise torques supporting the equilibrium roll/streak structure are produced by oblique waves properly collocated with the roll/streak structure.

4. The structural stability boundary for streak formation by this cooperative instability is not associated with modal instability of the streak and the finite amplitude equilibrium roll/streak structure is stable despite being highly inflectional in the spanwise direction. In fact, the inflectional mode acts to stabilize the streak.

A question often raised is whether the mechanism forming the roll/streak complex is essentially linear non-normal or essentially nonlinear[54, 87]. We find that both are involved in agreement with Kim and Lim[22]: the roll/streak is the optimal non-normal growth structure the growth of which is essentially related to non-normality of the linear shear flow dynamics while the destabilization of this roll/streak structure arises from the quadratically nonlinear Reynolds stresses. This forcing by perturbation Reynolds stresses of the non-normal optimal roll structure is an example of the mechanism of structure maintenance in turbulence by nonlinear scattering of perturbation energy into the linear non-normal optimally growing subspace. Because the non-normal roll/streak structure is so highly amplified, the energy scattered by nonlinear interaction into this structure dominates the structure of boundary layer turbulence.

Hamilton et al.[74] (HKW) obtain in an integration of a spatially constrained shear flow model what they identify as a regeneration mechanism for maintaining at finite amplitude the roll/streak complex. Their mechanism consists of a dynamic process of continual streak growth and decay associated [88] with forcing of the roll circulation by an unstable mode arising from spanwise inflectional streak instability. Their work addresses the problem of streak self-maintenance and presupposes that a streak of finite amplitude sufficient to produce an inflectional instability already exists. This work addresses the formation of streaks from arbitrarily small initial perturbations in FST. The finite amplitude equilibria we find, while inflectional, are modally stable and our streaks are maintained by the wave/mean flow interaction arising from a large subset of non-normal transient perturbation structures rather than by a single inflectional mode. In fact, as we have seen, the inflectional mode is primarily responsible for stabilizing the SSST streak instability at finite amplitude. Nevertheless, their numerical simulations agree with both observations and SSST in a number of other particulars including the importance of the streamwise roll as the linear non-normal optimally growing structure necessary for the formation of streaks and of Reynolds stresses in forcing the streamwise roll. HKW find it remarkable that turbulent perturbations "..produce additional streamwise vorticity in exactly the right places to augment the streamwise vortices."[74] but as we have seen, at least in the initial stages of streak formation, this coincidence is a necessary consequence of the existence of the SSST eigenmode and its nonlinear extension.

The SSST system provides analysis tools for obtaining a fundamental understanding of the underlying mechanisms of turbulence that can not be gained from interpretation of simulations alone so that we may say that SSST constitutes a theory of turbulence as distinct from a description of turbulence or an interpretation in dynamical terms of observations of turbulence. In this work we have used SSST to study the formation and maintenance of roll/streak structures in FST which is important in its own right but also as a component of the mechanism of bypass transition which typically proceeds from a pre-existing roll/streak structure.

X. CONCLUSION

Emergence of the roll/streak coherent structure in turbulent flow is a problem of great theoretical and practical importance. In this work we applied SSST to demonstrate a mechanism by which the roll/streak structure can arise from an emergent instability of roll/streak/turbulence interaction in boundary layer shear flow.

This emergent SSST instability giving rise to the roll/streak structure exploits the optimality of the non-normal roll/streak structure growth mechanism not by introducing an individual chance perturbation in cross-stream velocity but rather by organizing the ubiquitous torques associated with turbulent Reynolds stress divergence in the cross stream/spanwise plane to produce and maintain the optimal roll structure. This organization of the Reynolds stress by the streak resulting in forcing of the roll provides the missing coupling between the streak and roll that is required to produce instability from the non-normal growth process. At small amplitude the roll/streak structure grows exponentially as an eigenmode but at finite amplitude this growth is arrested and the structure approaches a nonlinear equilibrium. This mechanism of streak formation and equilibration is not related to instability of the perturbation dynamics of the streak and this cooperative SSST instability occurs in the absence of shear flow instability and the inflectional mode is found to stabilize the streak.

Acknowledgments

This work was supported by NSF ATM-0123389.

[1] L. Kelvin, "Stability of fluid motion: rectilinear motion of viscous fluid between two parallel planes," Phil. Mag. (5), **24**, 188–196 (1887).
[2] W. M. Orr, "Stability or instability of the steady motions of a perfect fluid," Proc. Roy. Irish Acad., **27**, 9–69 (1907).
[3] B. F. Farrell, "The initial growth of disturbances in a baroclinic flow," J. Atmos. Sci., **39**, 1663–1686 (1982).
[4] B. F. Farrell, "Transient growth of damped baroclinic waves," J. Atmos. Sci., **42**, 2718–2727 (1985).
[5] B. F. Farrell, "Optimal excitation of baroclinic waves," J. Atmos. Sci., **46**, 1193–1206 (1989).
[6] M. T. Landahl, "A note on an algebraic instability of inviscid parallel shear flows," J. Fluid Mech., **98**, 243 (1980).
[7] B. F. Farrell, "Optimal excitation of perturbations in viscous shear flow," Physics of Fluids, **31**, 2093–2102 (1988).
[8] R. Pierrehumbert, "Universal short-wave instability of two-dimensional eddies in an inviscid fluid," Phys. Rev. Lett., **57**, 2157–2159 (1986).
[9] B. Bayly, S. Orszag, and T. Herbert, "Instability mechanisms in shear-flow transition," Annual review of fluid mechanics, **20**, 359–391 (1988).
[10] K. M. Butler and B. F. Farrell, "Nonlinear equilibration of 2-d optimal perturbations in viscous shear flow," Phys. Fluids A, **6**, 2011–2020 (1994).
[11] K. M. Butler and B. F. Farrell, "Three-dimensional optimal perturbations in viscous shear flows," Phys. Fluids, **4**, 1637–1650 (1992).
[12] K. M. Butler and B. F. Farrell, "Optimal perturbations and streak spacing in turbulent shear flow," Phys. Fluids A, **3**, 774–776 (1993).
[13] B. F. Farrell and P. J. Ioannou, "Optimal excitation of three dimensional perturbations in viscous constant shear flow," Physics of Fluids, **5**, 1390–1400 (1993).
[14] B. F. Farrell and P. J. Ioannou, "Perturbation growth in shear flow exhibits universality," Physics of Fluids, **5**, 2298 (1993).
[15] S. C. Reddy and D. S. Henningson, "Energy growth in viscous shear flows," J. Fluid Mech., **252**, 209–238 (1993).
[16] L. N. Trefethen, A. E. Trefethen, S. C. Reddy, and T. A. Driscoll, "Hydrodynamic stability without eigenvalues," Science, **261**, 578–584 (1993).
[17] P. J. Schmid and D. S. Henningson, *Stability and Transition in Shear Flows* (Springer, New York, 2001).
[18] P. S. Klebanoff, K. D. Tidstrom, and L. M. Sargent, "The three-dimensional nature of boundary-layer instability," J. Fluid Mech., **12**, 1–34 (1962).
[19] W. Schoppa and F. Hussain, "Coherent structure dynamics in near-wall turbulence," Fluid Dynamics Research, **26**, 119–139 (2000).
[20] R. J. Adrian, "Hairpin vortex organization in wall turbulence," Physics of Fluids, **19**, 041301 (2007).
[21] X. Wu and P. Moin, "Direct numerical simulation of turbulence in a nominally zero-pressure-gradient flat-plate boundary layer," J. Fluid Mech., **630**, 5–41 (2009).
[22] J. Kim and J. Lim, "A linear process in wall bounded turbulent shear flows," Physics of Fluids, **12**, 1885–1888 (2003).
[23] W. Schoppa and F. Hussain, "Coherent structure generation in near-wall turbulence," J. Fluid Mech., **453**, 57–108 (2002).
[24] B. F. Farrell and P. J. Ioannou, "Stochastic forcing of the linearized Navier-Stokes equations," Phys. Fluids A, **5**, 2600–2609 (1993).
[25] B. F. Farrell and P. J. Ioannou, "Stochastic forcing of perturbation variance in unbounded shear and deformation flows," J. Atmos. Sci., **50**, 200–211 (1993).
[26] B. F. Farrell and P. J. Ioannou, "Variance maintained by stochastic forcing of non-normal dynamical systems associated with linearly stable shear flows," Phys. Rev. Lett., **72**, 1118–1191 (1994).
[27] B. F. Farrell and P. J. Ioannou, "Perturbation structure and spectra in turbulent channel flow," Theor. Comput. Fluid Dyn., **11**, 215–227 (1998).
[28] B. F. Farrell and P. J. Ioannou, "Turbulence supresssion by active control," Physics of Fluids, **8**, 1257–1268 (1998).
[29] B. Bamieh and M. Dahleh, "Energy amplification in channel flows with stochastic excitation," Physics of Fluids, **13**, 3258–3269 (2001).
[30] M. Jovanovic and B. B., "Componentwise energy amplification in channel flows," J. Fluid Mech., **534**, 145–183 (2005).
[31] J. Hoepffner and L. Brandt, "Stochastic approach to the receptivity problem applied to bypass transition in boundary layers," Physics of Fluids, **20**, 024108 (2008).
[32] Y. Hwang and C. Cossu, "Amplification of coherent structures in the turbulent Couette flow: an input-output analysis at low Reynolds number," J. Fluid Mech., **643**, 333–348 (2010).
[33] B. J. McKeon, A. Papachristodoulou, B. Bamieh, and D. J. C., "A streamwise constant model of turbulence in plane Couette flow," J. Fluid Mech., (To appear) (2010).
[34] Y. Hwang and C. Cossu, "Linear non-normal energy amplification of harmonic and stochastic forcing in the turbulent channel flow," J. Fluid Mech., doi:10.1017/S0022112010003629, Published online by Cambridge University Press 22 September 2010.
[35] A. P., M. Berggren, and D. S. Henningson, "Optimal disturbances and bypass transition in boundary layers," Physics of

Fluids, **11**, 134 (1999).
[36] G. Brown and A. Thomas, "Large structure in a turbulent boundary layer," Physics of Fluids, **20**, 243–252 (1977).
[37] W. R. C. Phillips, Z. Wu, and J. L. Lumley, "On the formation of longitudinal vortices in a turbulent boundary layer over wavy terrain," Journal of Fluid, **326**, 321–341 (1996).
[38] D. J. Benney, "A non-linear theory for oscillations in a parallel flow," J. Fluid Mech., **10**, 209–236 (1960).
[39] P. S. Jang, D. J. Benney, and R. L. Gran, "On the origin of streamwise vortices in a turbulent boundary layer," J. Fluid Mech., **169**, 109–123 (1986).
[40] J. Komminaho, A. Lundbladh, and A. Johansson, "Very large structures in plane turbulent Couette flow," J. Fluid Mech., **320**, 259–285 (1996).
[41] B. F. Farrell and P. J. Ioannou, "Formation of jets by baroclinic turbulence," J. Atmos. Sci., **65**, 3353–3375 (2008).
[42] E. N. Parker, "Hydromagnetic dynamo models," Astrophys. J., **122**, 293314 (1955).
[43] B. F. Farrell and P. J. Ioannou, "Structural stability of turbulent jets," J. Atmos. Sci., **60**, 2101–2118 (2003).
[44] B. F. Farrell and P. J. Ioannou, "Structure and spacing of jets in barotropic turbulence," J. Atmos. Sci., **64**, 3652–3665 (2007).
[45] B. F. Farrell and P. J. Ioannou, "A stochastic structural stability theory model of the drift wave-zonal flow system," Physics of Plasmas, **16**, 112903 (2009).
[46] B. F. Farrell and P. J. Ioannou, "Stochastic dynamics of baroclinic waves," J. Atmos. Sci., **50**, 4044–4057 (1993).
[47] B. F. Farrell and P. J. Ioannou, "Generalized stability. Part I: Autonomous operators," J. Atmos. Sci., **53**, 2025–2040 (1996).
[48] T. DelSole and B. F. Farrell, "The quasi-linear equilibration of a thermally mantained stochastically excited jet in a quasigeostrophic model," J. Atmos. Sci., **53**, 1781–1797 (1996).
[49] T. DelSole, "Stochastic models of quasigeostrophic turbulence," Surveys in Geophysics, **25**, 107–194 (2004).
[50] B. F. Farrell and P. J. Ioannou, "Emergence of jets from turbulence in the shallow-water equations on an equatorial beta-plane," J. Atmos. Sci., **66**, 3197–3207 (2009).
[51] B. F. Farrell and P. J. Ioannou, "A theory of baroclinic turbulence," J. Atmos. Sci., **66**, 2444–2454 (2009).
[52] E. Mazzucato, S. Batha, M. Beer, and M. Bell, "Turbulent fluctuations in TFTR configurations with reversed magnetic shear," Phys. Rev. Lett., **77**, 3145 – 3148 (1996).
[53] P. J. Schmid and D. S. Henningson, "A new mechanism for rapid transition involving a pair of oblique waves," Physics of Fluids A: Fluid Dynamics, **4**, 1986–1989 (1992).
[54] F. Waleffe, "Transition in shear flows. Nonlinear normality versus non- normal linearity," Physics of Fluids, **7**, 3060 (1995).
[55] J.-P. Laval, B. Dubrulle, and J. C. McWilliams, "Langevin models of turbulence: Renormalization group, distant interaction algorithms or rapid distortion theory?" Physics of Fluids, **15**, 1327–1339 (2003).
[56] T. R. Bewley and S. Liu, "Optimal and robust control and estimation of linear paths to transition," J. Fluid Mech., **365**, 23–57 (1998).
[57] J. Kim and T. R. Bewley, "A linear systems approach to flow control," Annu. Rev. Fluid Mech., **39**, 383–417 (2007).
[58] M. Hogberg, T. R. Bewley, and D. S. Henningson, "Linear feedback control and estimation of transition in plane channel flow," J. Fluid Mech., **481**, 149–175 (2003).
[59] M. Hogberg, T. R. Bewley, and D. S. Henningson, "Relaminarization of Re=1000 turbulence using linear state-feedback control," Physics of Fluids, **15**, 3572–3575 (2003).
[60] B. F. Farrell and P. J. Ioannou, "Stochastic dynamics of the midlatitude atmospheric jet," J. Atmos. Sci., **52**, 1642–1656 (1995).
[61] T. DelSole, "Can quasigeostrophic turbulence be modeled stochastically?" J. Atmos. Sci., **53**, 1617–1633 (1996).
[62] J. S. Whitaker and P. D. Sardeshmukh, "A linear theory of extratropical synoptic eddy statistics," J. Atmos. Sci., **55**, 237–258 (1998).
[63] Y. Zhang and I. M. Held, "A linear stochastic model of a GCM's midlatitude storm tracks," J. Atmos. Sci., **56**, 3416–3435 (1999).
[64] T. DelSole, "A simple model for transient eddy momentum fluxes in the upper troposphere," J. Atmos. Sci., **58**, 3019–3035 (2001).
[65] Discussion of application of the ergodic assumption in this context with examples of convergence can be found in FI2003[43].
[66] G. Branstator and J. D. Opsteegh, "Free solutions of the barotropic vorticity equation," J. Atmos. Sci., **46**, 1799–1814 (1989).
[67] J. Marshall and F. Molteni, "Toward a dynamical understanding of planetary-scale flow regimes," J. Atmos. Sci., **50**, 1792– (1993).
[68] M. Nagata, "Three-dimensional finite-amplitude solutions in plane couette flow: bifurcation from infinity," J. Fluid Mech., **217**, 519–527 (1990).
[69] F. Waleffe, "Homotopy of exact coherent structures in plane shear flows," Physics of Fluids, **15**, 1517–1534 (2003).
[70] J. Gibson, J. Halcrow, and P. Cvitanović, "Visualizing the geometry of state space in plane couette flow," J. Fluid Mech., **611**, 107–130 (2008).
[71] L. Rayleigh, "On the stability, or instability, of certain fluid motions," Proc. London Math. Soc., **11**, 57–70 (1880).
[72] The stability operator $\mathcal{L}$ is discussed more fully in Farrell&Ioannou[43].
[73] V. A. Romanov, "Stability of plane-parallel Couette flow," Funct. Anal. Appl., **7**, 137 (1973).
[74] K. Hamilton, J. Kim, and F. Waleffe, "Regeneration Mechanisms of Near-Wall Turbulence Structures," J. Fluid Mech., **287**, 317–348 (1995).
[75] J. Jimenez and M. P., "The minimal flow unit in near wall turbulence," J. Fluid Mech., **225**, 213–240 (1991).

[76] F. Waleffe, "Hydrodynamic stability and turbulence:Beyond transients to a self-sustaining proccess," Stud. Appl. Maths, **95**, 319–343 (1995).
[77] F. Waleffe, "On a self-sustaining process in shear flows," Phys. Fluids A, **9**, 883–900 (1997).
[78] S. C. Reddy, P. J. Schmid, J. S. Baggett, and D. S. Henningson, "On the stability of streamwise streaks and transition thresholds in plane channel flows," J. Fluid Mech., **365**, 269–303 (1998).
[79] K. J. A. Westin, A. V. Boiko, B. G. B. Klingmann, V. V. Kozlov, and P. H. Alfredsson, "Experiments in a boundary layer subjected to free stream turbulence. part 1. boundary layer structure and receptivity," J. Fluid Mech., **281**, 193 (1994).
[80] H. Jeffreys, "The function of cyclones in the general circulation," in *Proces.-Verbaux de l'Association de Meteorologie* (UGGI (Lisbon), Part II, 1933) pp. 219–230.
[81] V. Starr, *Physics of negative viscosity phenomena* (McGraw Hill, New York, 1968) p. 256.
[82] W. A. Robinson, "Does eddy feedback sustain variability in the zonal index?" J. Atmos. Sci., **53**, 3556–3569 (1996).
[83] D. C. Hill, "Adjoint systems and their role in the receptivity problem for boundary layers," J. Fluid Mech., **292**, 183–204 (1995).
[84] K. Moffatt, "The interaction of turbulence with strong wind shear," in *Atmospheric Turbulence and Radio Wave Propagation*, edited by A. M. Yaglom and V. I. Tatarskii (Nauka, Moscow, 1967).
[85] J. Kim, P. Moin, and R. Moser, "Turbulence statistics in fully developed channel flow at low Reynolds number," J. Fluid Mech., **177**, 133–166 (1987).
[86] N. Hutchins and I. Marusic, "Evidence of very long meandering features in the logarithmic region of turbulent boundary layers," J. Fluid Mech., **579**, 1–28 (2007).
[87] D. S. Henningson, "Comment on "Transition in shear flows. Nonlinear normality versus non-normal linearity" [Phys. Fluids 7, 3060 (1995)]," Physics of Fluids, **8**, 2257–2258 (1996).
[88] F. Waleffe and J. Kim, "How streamwise rolls and streaks self-sustain in a shear flow," in *Self-sustaining mechanisms of wall turbulence(A 98-17710 03-34)*.
[89] Discussion of application of the ergodic assumption in this context with examples of convergence can be found in FI2003[43].
[90] The stability operator $\mathcal{L}$ is discussed more fully in Farrell&Ioannou[43].

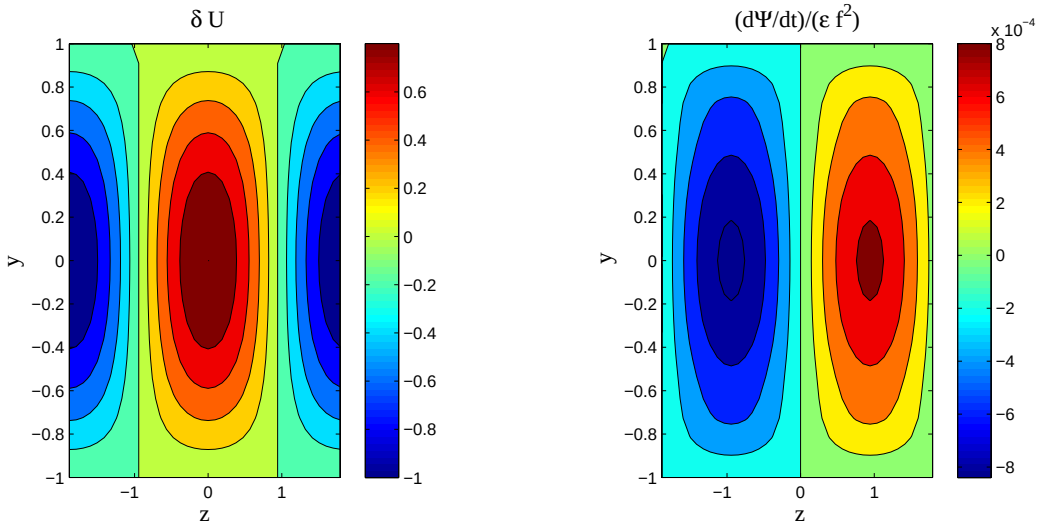

FIG. 1: (Color online) Left: Streamwise flow perturbation $\delta U = \epsilon \cos(\pi y/(2L_y)) \cos(2\pi z/Lz)$ imposed on a background Couette flow to examine the mechanism of turbulent Reynolds stress organization. Right: Resulting equilibrium Reynolds stress divergence induced tendency in the cross-stream/spanwise streamfunction, $d\Psi/dt$, normalized by the mean flow perturbation amplitude, ϵ, and the square of the STM excitation parameter parameter, f. Imposition of a spanwise perturbation breaks the spanwise symmetry of the Couette flow producing a coherent streamwise torque proportional to both the mean flow perturbation and to the eddy field variance. The channel dimensions are $L_y = 1$, $L_z = 1.2\pi$, the Reynolds number is $R = 400$, and the eddy field is at streamwise wavenumber $k = 2\pi/(1.75\pi)$.

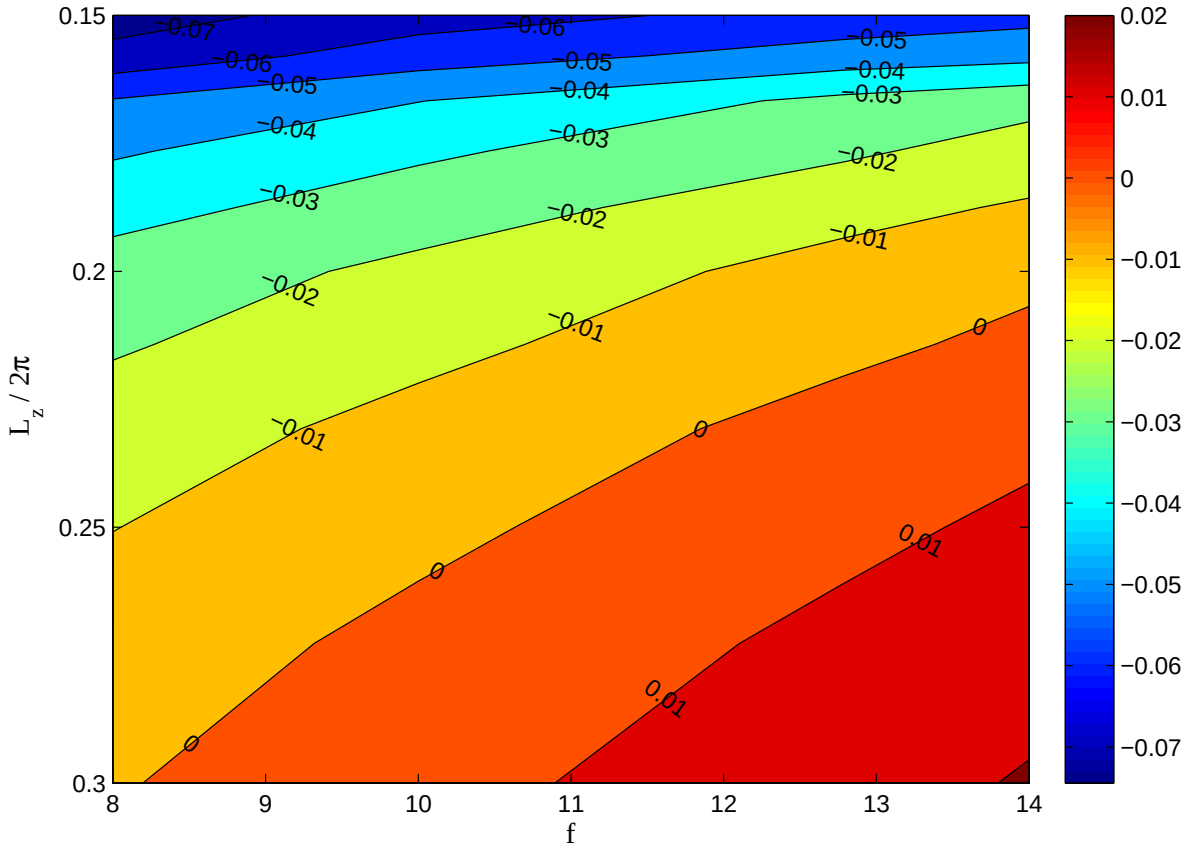

FIG. 2: (Color online) Growth rate of the most unstable eigenfunction of the SSST system linearized about the spanwise uniform equilibrium as a function of STM excitation parameter, f, and spanwise channel width, L_z. Channel width $L_z/(2\pi) = 3/10$, as used in the example of Fig. 3, lie on the abscissa of this plot. Channels with spanwise width $L_z/(2\pi) < 0.205$ are stable. The perturbation field comprises a single wavenumber, $k = 1$. The Reynolds number is $R = 400$.

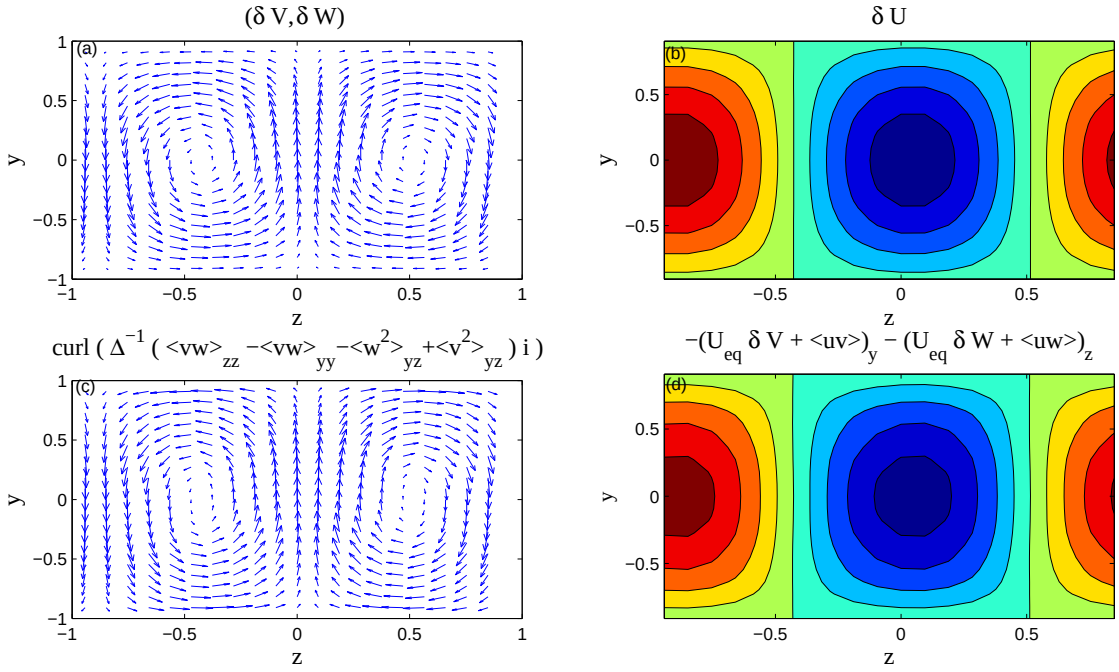

FIG. 3: (Color online) The most unstable eigenfunction of the SSST system linearized about the structurally unstable equilibrium with no spanwise variation at STM excitation parameter $f = 12.8$. The growth rate of this eigenfunction is $\lambda = 0.0166$. (a): streamwise mean cross-stream/spanwise velocity vectors $(\delta V, \delta W)$ in the cross-stream/spanwise plane. (b): streamwise mean streamwise velocity δU associated with the same eigenfunction (negative values dashed). The ratio of the maxima of the fields $(\delta U, \delta V, \delta W)$ is $(1, 0.06, 0.03)$. The unstable eigenfunction also has a perturbation covariance component, δC, the effect of which is indicated by the acceleration these perturbations induce in the corresponding velocities (cf. equations (4) and (6)): (c): $(\delta\dot{V}, \delta\dot{W})$. (d): $\delta\dot{U}$. Parameters are $k = 1$, $Lz/(2\pi) = 0.3$ and $R = 400$.

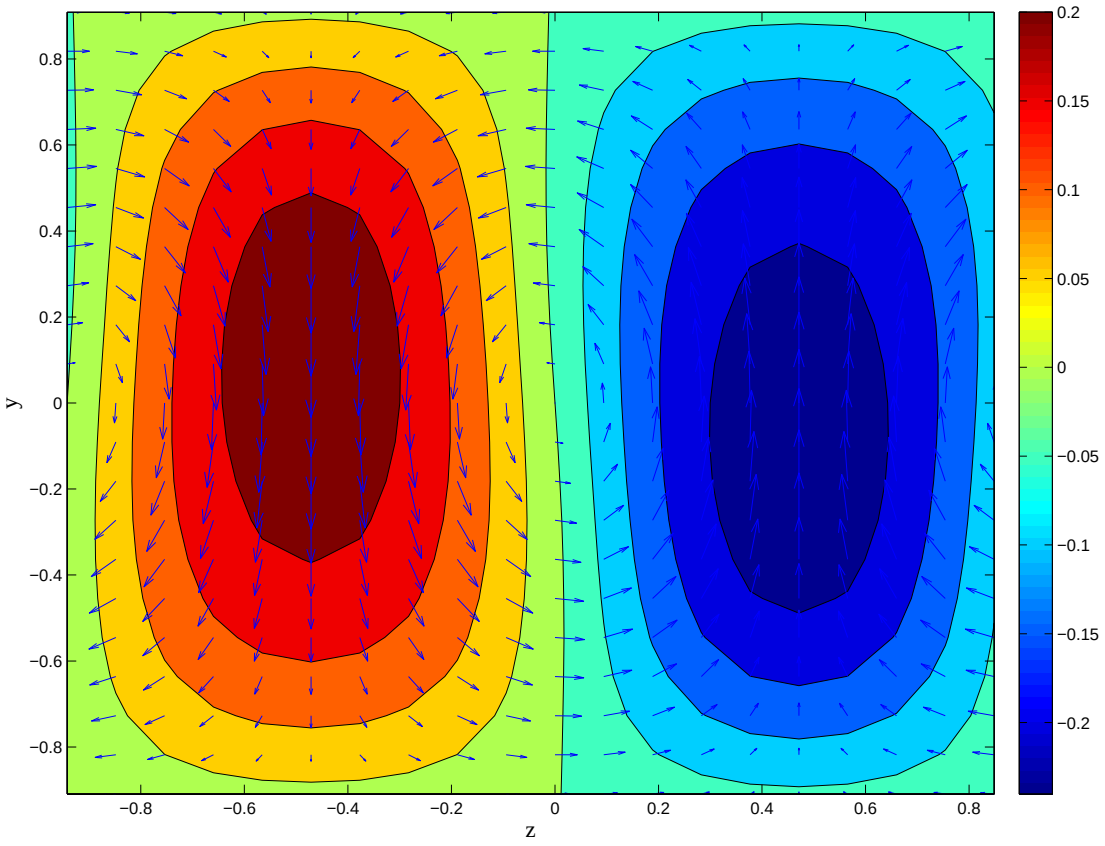

FIG. 4: (Color online) Finite amplitude equilibrium roll/streak structure at STM excitation parameter $f = 12.8$. Shown are contours of the streak velocity, U_s, and velocity vectors (V, W) of the roll circulation that equilibrates from the most unstable eigenfunctions shown in Fig. 3.

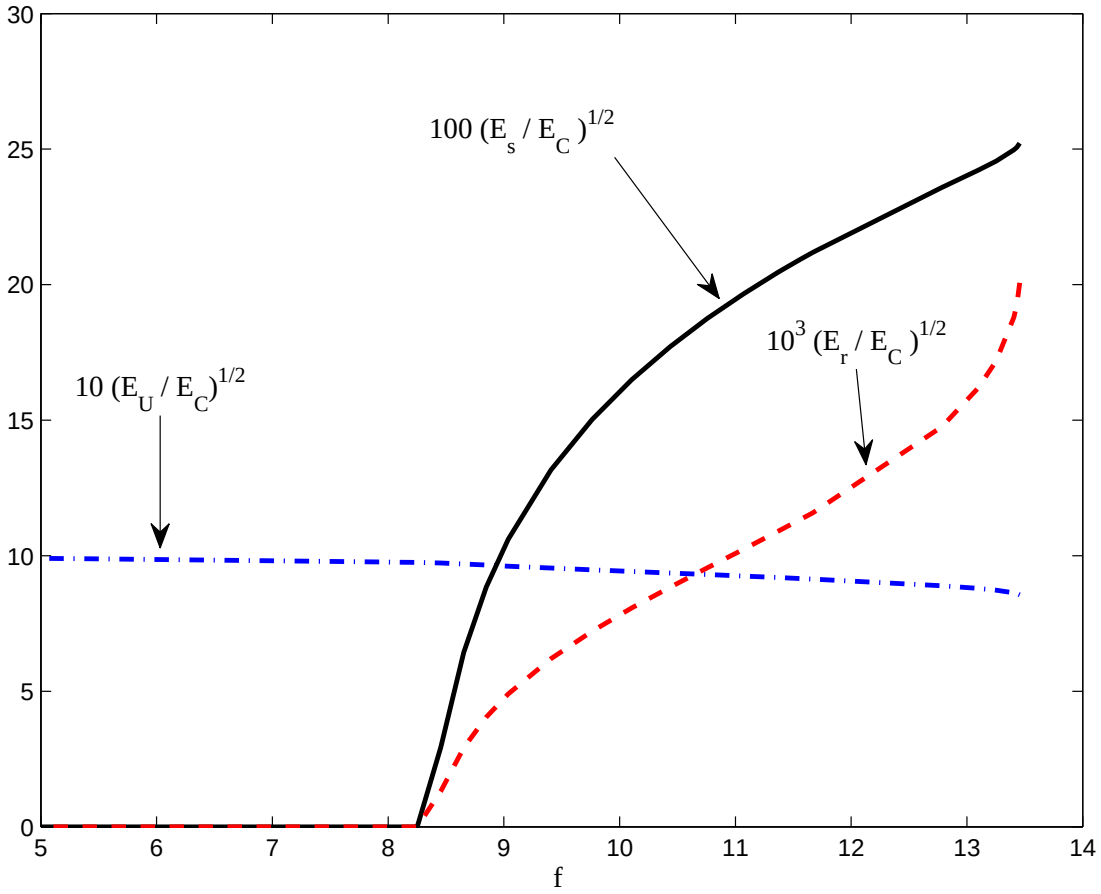

FIG. 5: (Color online) Roll/streak equilibria as a function of the STM excitation parameter, f. At the critical turbulence level corresponding to $f_c = 8.25$ the spanwise independent equilibria bifurcate to spanwise dependent roll/streak equilibria. Shown are RMS streak amplitude (continuous), RMS roll amplitude (dashed), and RMS streamwise mean flow amplitude (dash-dot) normalized by the RMS velocity of the unperturbed Couette flow, $\sqrt{E_C}$. The Reynolds number is $R = 400$ and the perturbation field wavenumber is $k = 1$.

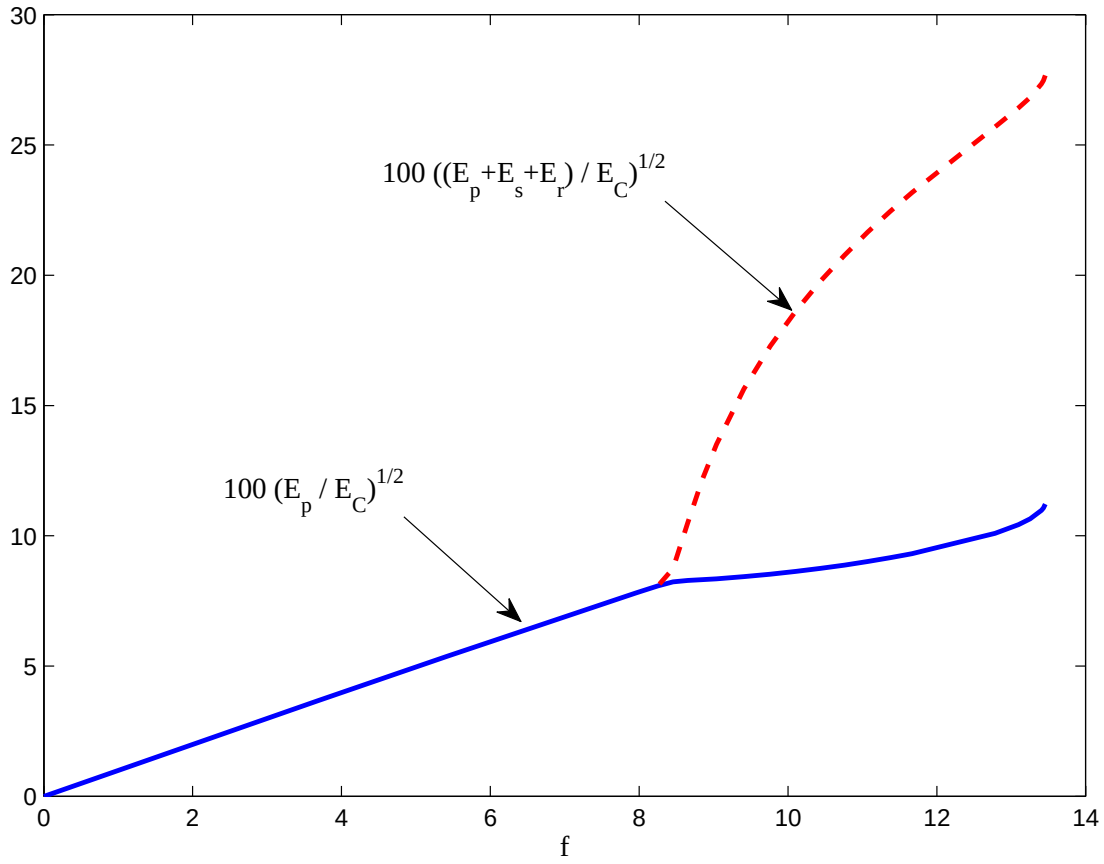

FIG. 6: (Color online) RMS velocity of the sum of perturbation, roll, and streak components $\sqrt{(E_p + E_m + E_s)/E_C}$ (dashed), and of the perturbation alone $\sqrt{E_p/E_C}$ (solid) normalized by the Couette RMS velocity, $\sqrt{E_C}$, as a function of STM excitation parameter, f. These curves diverge at the bifurcation STM excitation parameter, $f_c = 8.25$, at which the roll and the streak emerge. As the STM excitation parameter increases beyond f_c the roll/streak complex rapidly increases in contribution to the total energy while the perturbation RMS velocity remains near 10% of the mean velocity. Parameters as in Fig. 3.

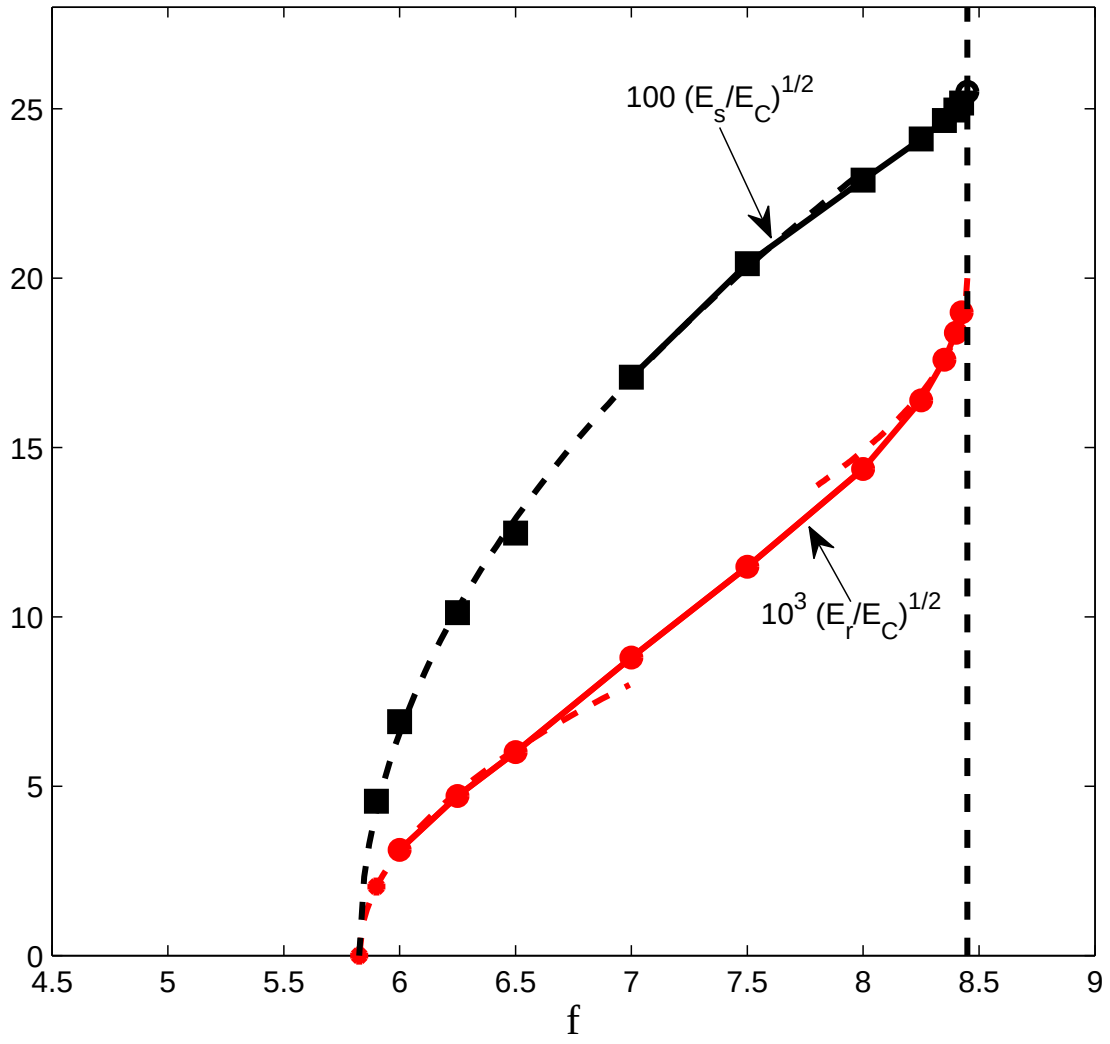

FIG. 7: (Color online) Bifurcation diagram of the roll/streak structure as a function of STM excitation parameter, f. At $f_c = 5.825$ the spanwise uniform equilibrium bifurcates to a spanwise dependent roll/streak equilibrium. Shown as a function of f is normalized streak strength, $100(E_s/E_C)^{1/2}$ (squares) and normalized roll strength, $10^3(E_r/E_C)^{1/2}$ (circles). The dashed line indicates the $\sqrt{f - f_c}$ dependence of a second order bifurcation. The stable equilibria extend up to $f_u = 8.45$; at which point the perturbation stable roll/streak equilibrium becomes structurally unstable. The dashed line indicates the $\sqrt{f_u - f}$ dependence of a second order bifurcation. Parameters correspond to the HKW channel: length $L_x = 1.75\pi$, spanwise width $L_z = 1.2\pi$, half cross-stream height $L_y = 1.0$ and the Reynolds number is $R = 400$. The perturbation streamwise wavenumber, $k = 1.143$, corresponds to the gravest mode in the channel.

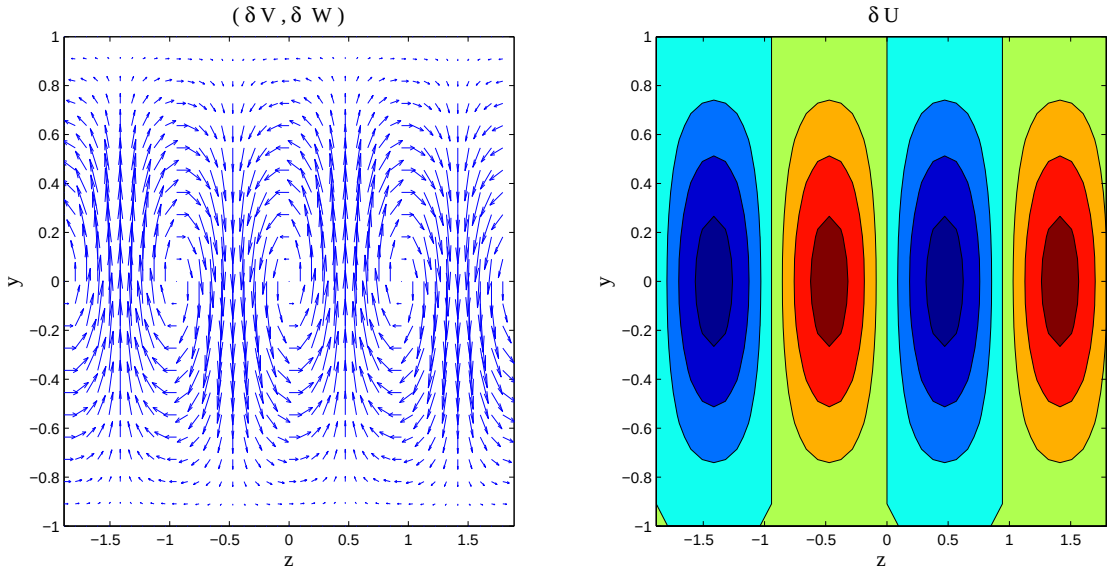

FIG. 8: (Color online) The most unstable eigenfunction of the SSST system linearized about the structurally unstable equilibrium with no spanwise variation at STM excitation parameter $f = 8.4$. The growth rate of this mode is $\lambda = 0.014$. Left: streamwise mean cross-stream/spanwise velocity vectors $(\delta V, \delta W)$ in the cross-stream/spanwise plane. Right: streamwise mean streamwise velocity δU. The ratio of the maxima of the fields $(\delta U, \delta V, \delta W)$ is $(1, 0.06, 0.03)$. Parameters correspond to the HKW channel: length $L_x = 1.75\pi$, spanwise width $L_z = 1.2\pi$, half cross-stream height $L_y = 1.0$ and the Reynolds number is $R = 400$. The perturbation streamwise wavenumber, $k = 1.143$, corresponds to the gravest mode in the channel.

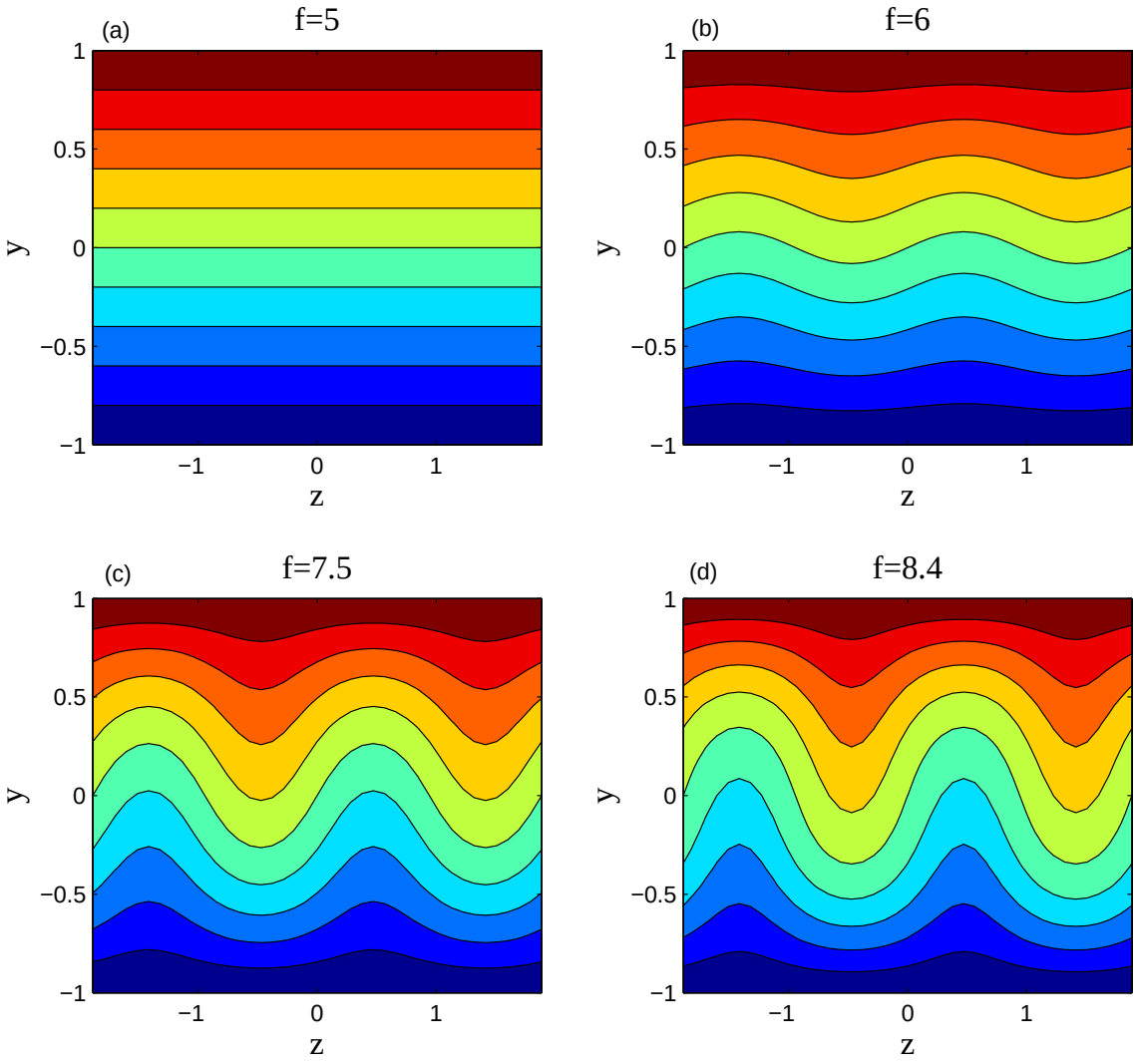

FIG. 9: (Color online) Streamwise mean velocity in the (y, z) plane for the equilibria at various STM excitation parameter values, f. (a): at STM excitation parameter value $f = 5$ the equilibrium is spanwise uniform and there is no associated roll/streak. (b): At $f = 6$ the spanwise independent flow is structurally unstable and the associated equilibrium flow has a weak streak with associated roll/streak. (c): The equilibrium at $f = 7.5$. (d): The equilibrium at $f = 8.4$. All these equilibria are perturbation stable. Parameters correspond to the HKW channel: length $L_x = 1.75\pi$, spanwise width $L_z = 1.2\pi$, half cross-stream height $L_y = 1.0$ and the Reynolds number is $R = 400$. The perturbation streamwise wavenumber, $k = 1.143$, corresponds to the gravest mode in the channel.

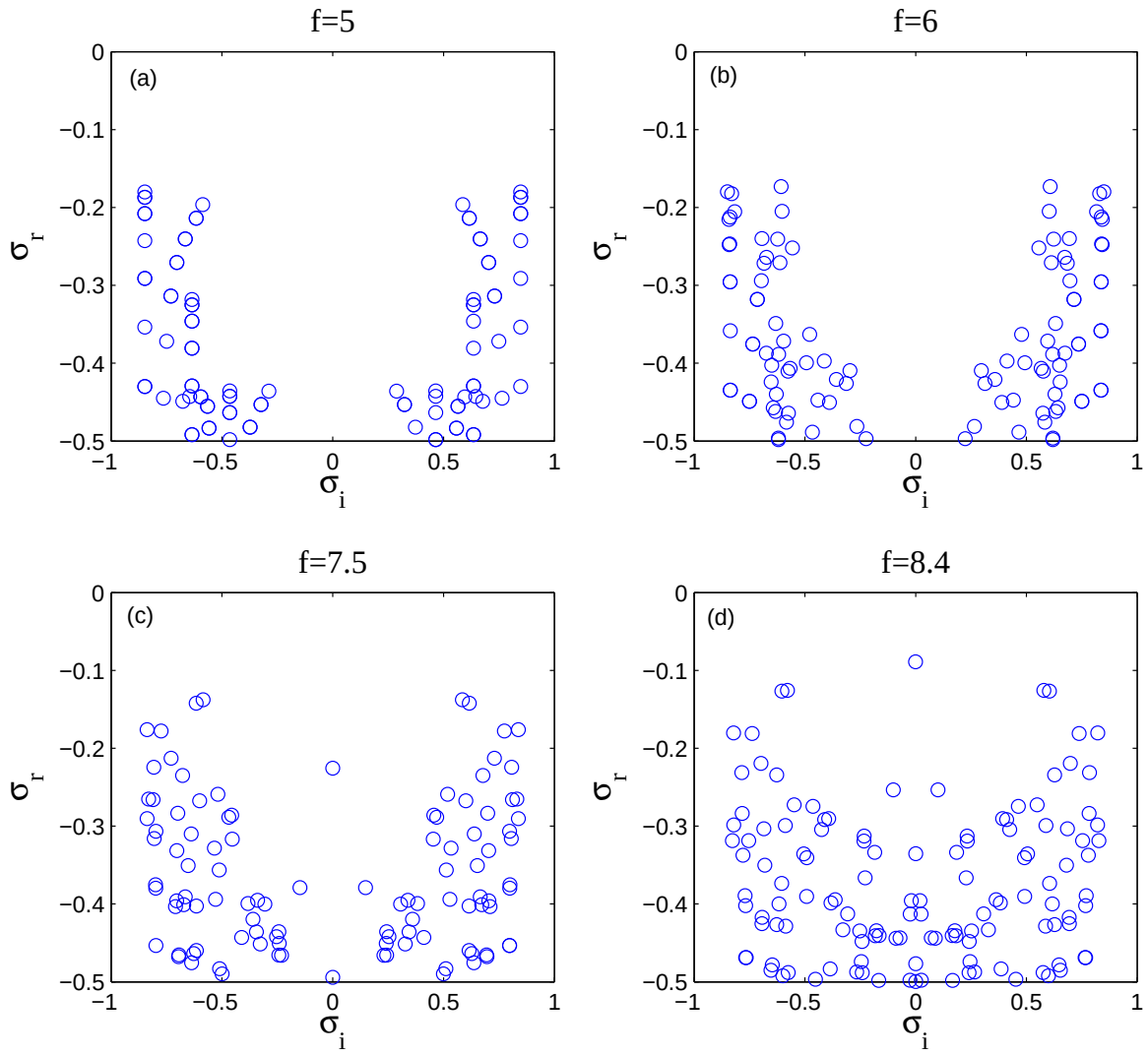

FIG. 10: (Color online) The least stable eigenvalues (σ_r, σ_i) of the operators $\mathbf{A}_k$ that govern the perturbation stability of the equilibrium flows shown in Fig. 9. All the flows are perturbation stable. Note the emergence of a mode with $\sigma_r = 0$ as the streak increases in magnitude. Parameters correspond to the HKW channel: length $L_x = 1.75\pi$, spanwise width $L_z = 1.2\pi$, half cross-stream height $L_y = 1.0$ and the Reynolds number is $R = 400$. The perturbation streamwise wavenumber, $k = 1.143$, corresponds to the gravest mode in the channel.

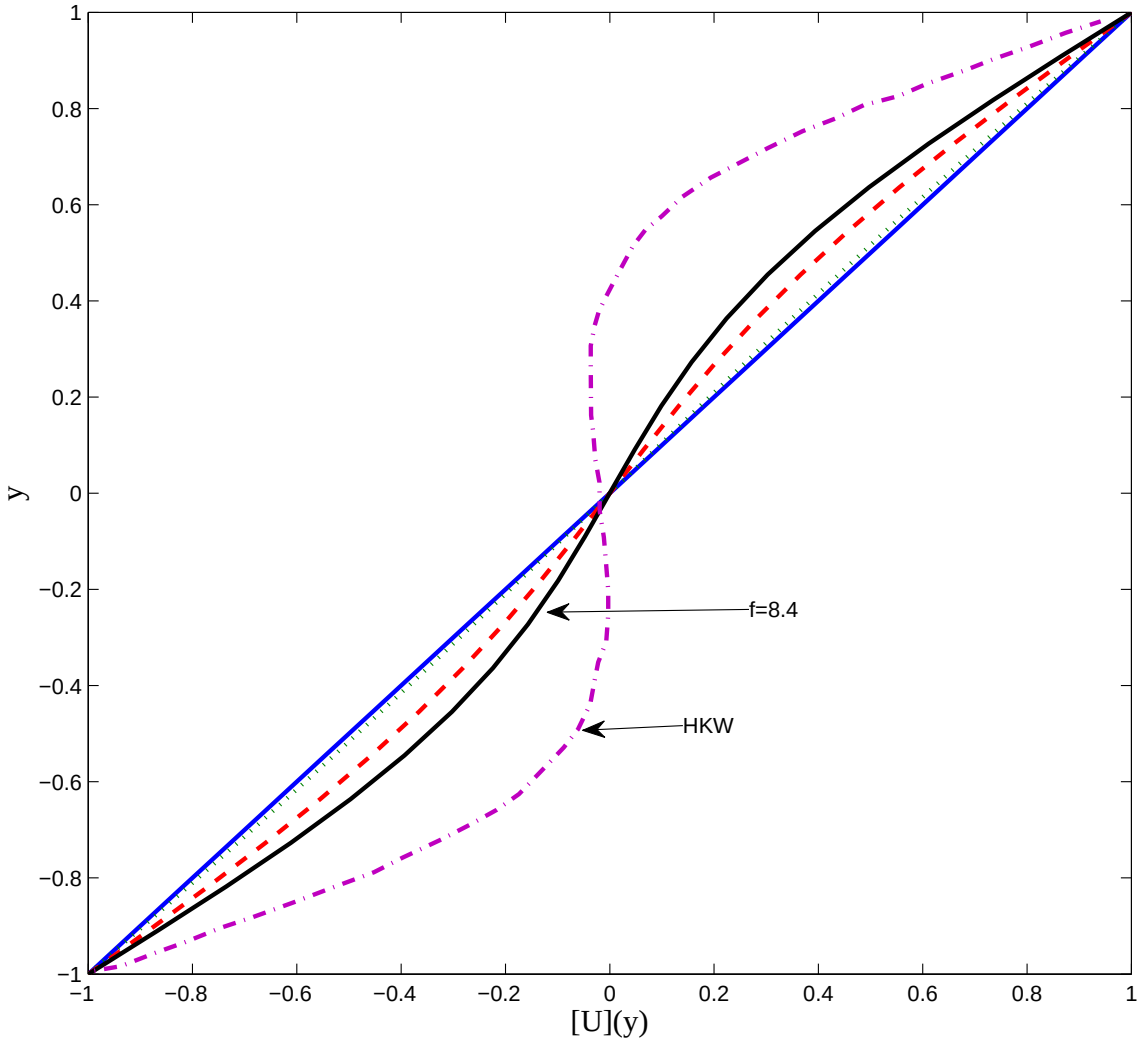

FIG. 11: (Color online) The spanwise averaged streamwise flow, $[U](y)$, for the SSST equilibria for STM excitation parameter $f = 8.4$ (solid), $f = 7.5$ (dashed), $f = 6$ (dotted) as shown in Fig. 9. Also shown for comparison is the time and spanwise mean under turbulent conditions (dash-dot) as well as the laminar Couette flow. The laminar roll/streak equilibrium at $f = 8.4$ produces dissipation $1.4D_C$, where D_c is the dissipation in Couette flow, and the half channel width in wall units at this value of f is $L_y = 24y^+$. Parameters correspond to the HKW channel: length $L_x = 1.75\pi$, spanwise width $L_z = 1.2\pi$, half cross-stream height $L_y = 1.0$ and the Reynolds number is $R = 400$. The perturbation streamwise wavenumber, $k = 1.143$, corresponds to the gravest mode in the channel.

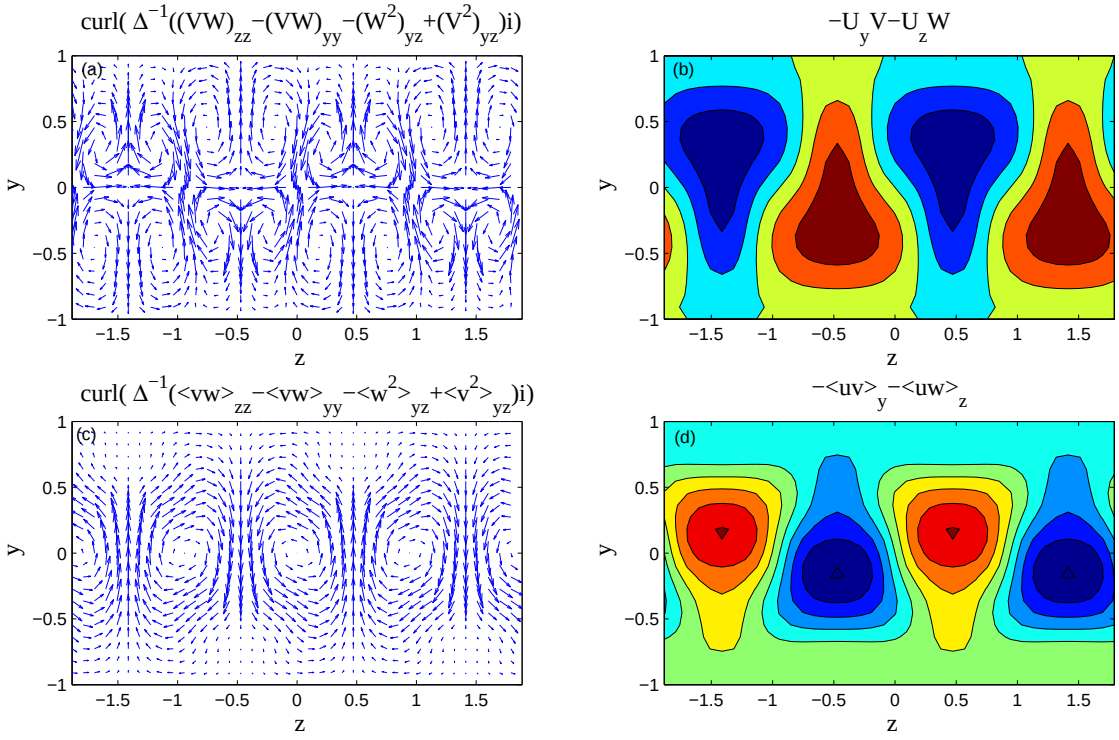

FIG. 12: (Color online) For the equilibrium shown in Fig. 9d; (a): acceleration vectors, $(\dot{V}, \dot{W})$, of the streamwise mean roll circulation induced by the mean velocity field, the maximum $\dot{V}$ is 10^{-4}. (b): acceleration of the mean streamwise flow, $\dot{U}$, induced by the streamwise mean roll circulation, the maximum $\dot{U}$ is 10^{-2}, mainly due to the lift-up mechanism. (c): acceleration vectors, $(\dot{V}, \dot{W})$, of the streamwise mean roll circulation induced by the eddy field, the maximum $\dot{V}$ is 10^{-3}. (d): acceleration of the mean streamwise flow, $\dot{U}$, induced by the eddy field, the maximum $\dot{U}$ is 10^{-2}. The eddy field decelerates the streaks. Parameters correspond to the HKW channel: length $L_x = 1.75\pi$, spanwise width $L_z = 1.2\pi$, half cross-stream height $L_y = 1.0$ and the Reynolds number is $R = 400$. The perturbation streamwise wavenumber, $k = 1.143$, corresponds to the gravest mode in the channel.

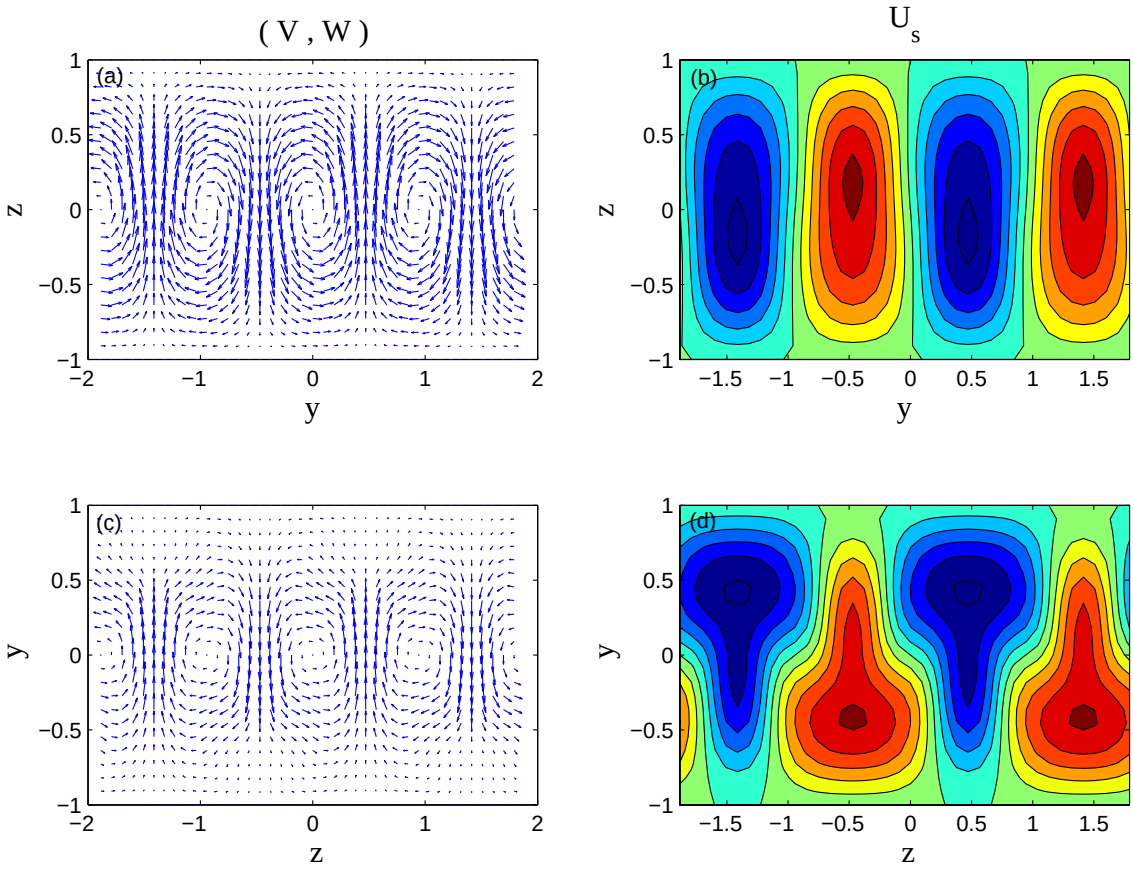

FIG. 13: (Color online) For the equilibrium shown in Fig. 9d; (a): Roll vector velocity (V, W) at equilibrium, the maximum V velocity is 0.02 and the maximum W velocity is 0.009. (b): Streak velocity $U_s = U - [U]$ at equilibrium, the maximum velocity is 0.26. (c): mean roll acceleration vectors induced by both the mean and eddy fields given by $\nabla \times (\Delta^{-1}((VW + < vw >)_{zz} - (VW + < vw >)_{yy} - (W^2 + < w^2 >)_{yz} + (V^2 + < v^2 >)_{yz})i)$. The roll circulation is maintained against friction by the eddy field. (d): mean streamwise acceleration induced by both the mean and eddy fields $-(UV + < uv >)_y - (UW + < uw >)_z$.
The mean streamwise flow is maintained against friction by the lift up mechanism.

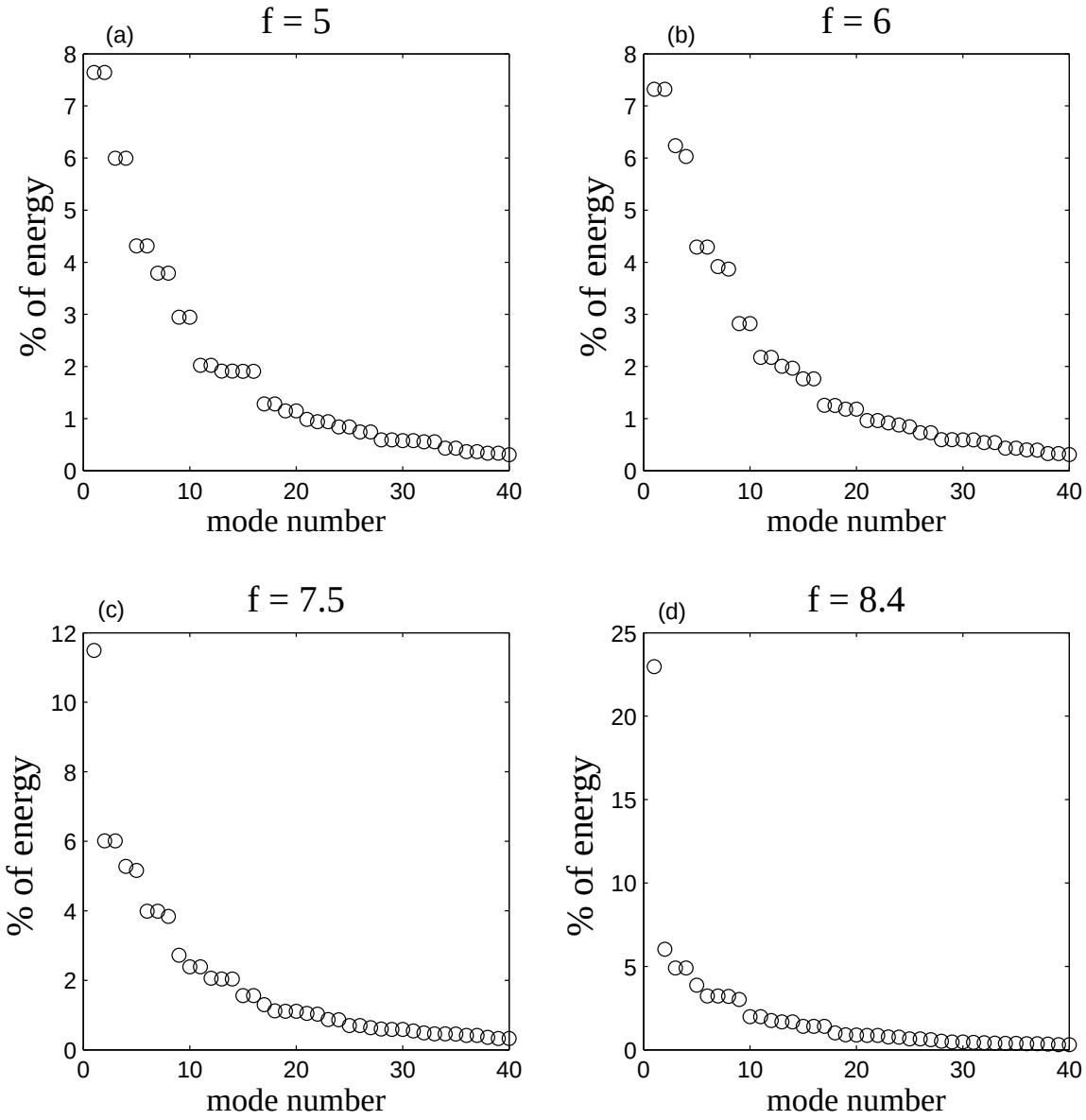

FIG. 14: (Color online) Percentage contribution of the leading EOF's of the equilibrium covariance to the total eddy mean energy maintained by the equilibria shown in Fig. 9.

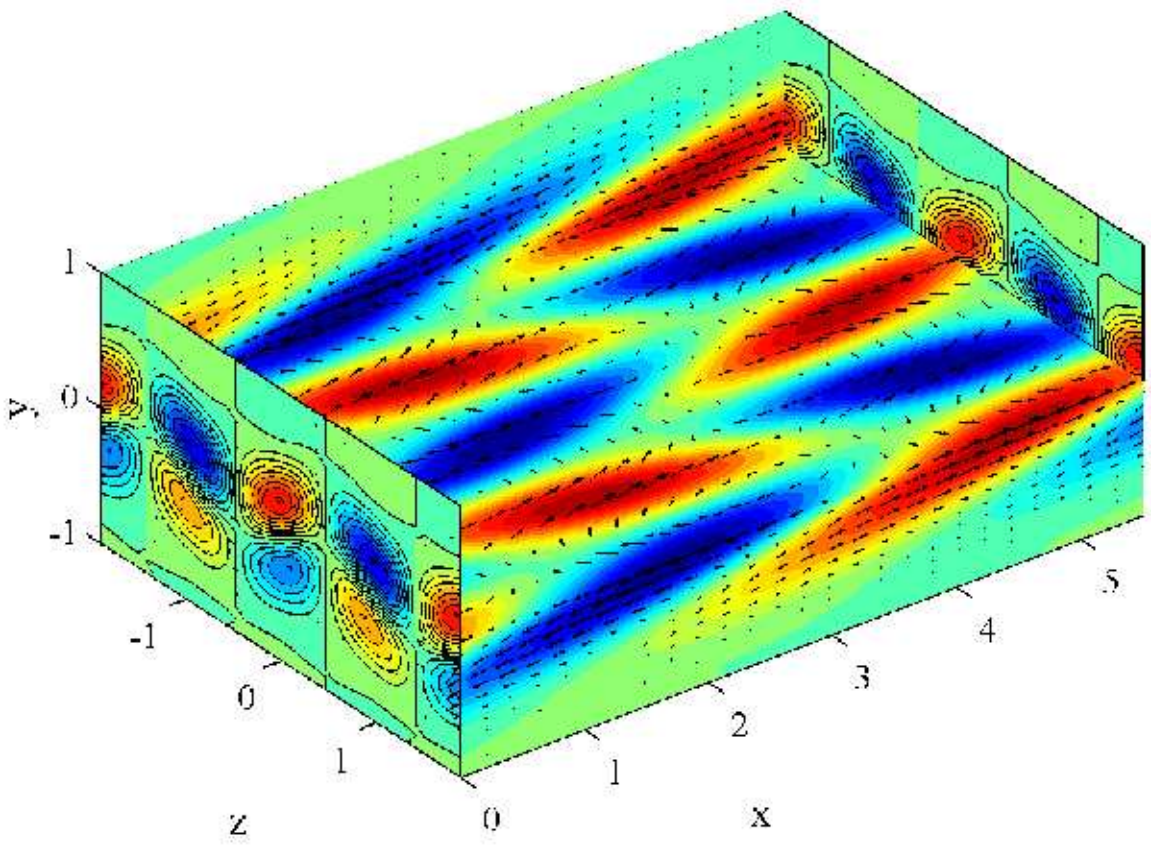

FIG. 15: (Color online) Velocity field of the gravest EOF accounting for 24% of the eddy energy for STM excitation parameter $f = 8.4$. Velocity vectors are shown with contours of streamwise velocity. Parameters correspond to the HKW channel: length $L_x = 1.75\pi$, spanwise width $L_z = 1.2\pi$, half cross-stream height $L_y = 1.0$ and the Reynolds number is $R = 400$. The perturbation streamwise wavenumber, $k = 1.143$, corresponds to the gravest mode in the channel.

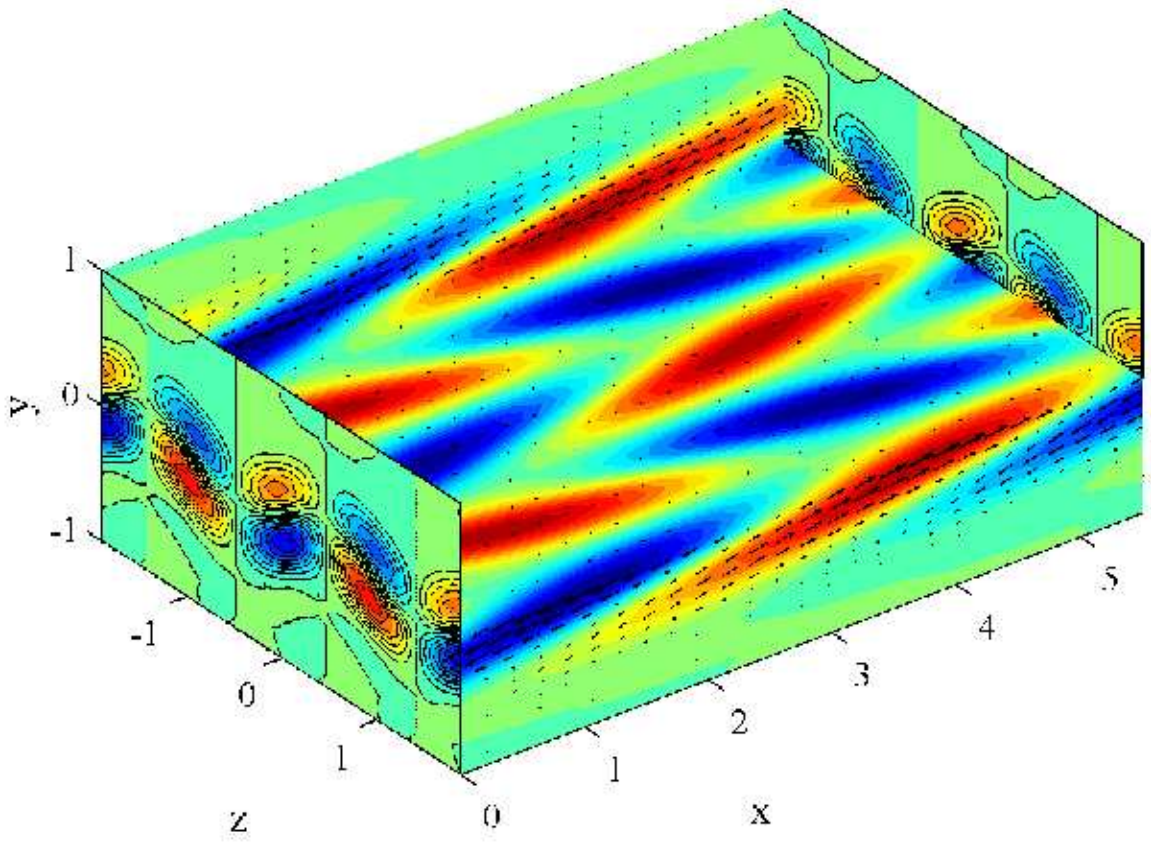

FIG. 16: (Color online) Velocity field of the least stable mode with eigenvalue ($\sigma_r = -0.017$, $\sigma_i = 0$), for the equilibrium at STM excitation parameter $f = 8.4$. Velocity vectors are shown with contours of streamwise velocity. Parameters are as in Fig. 15.

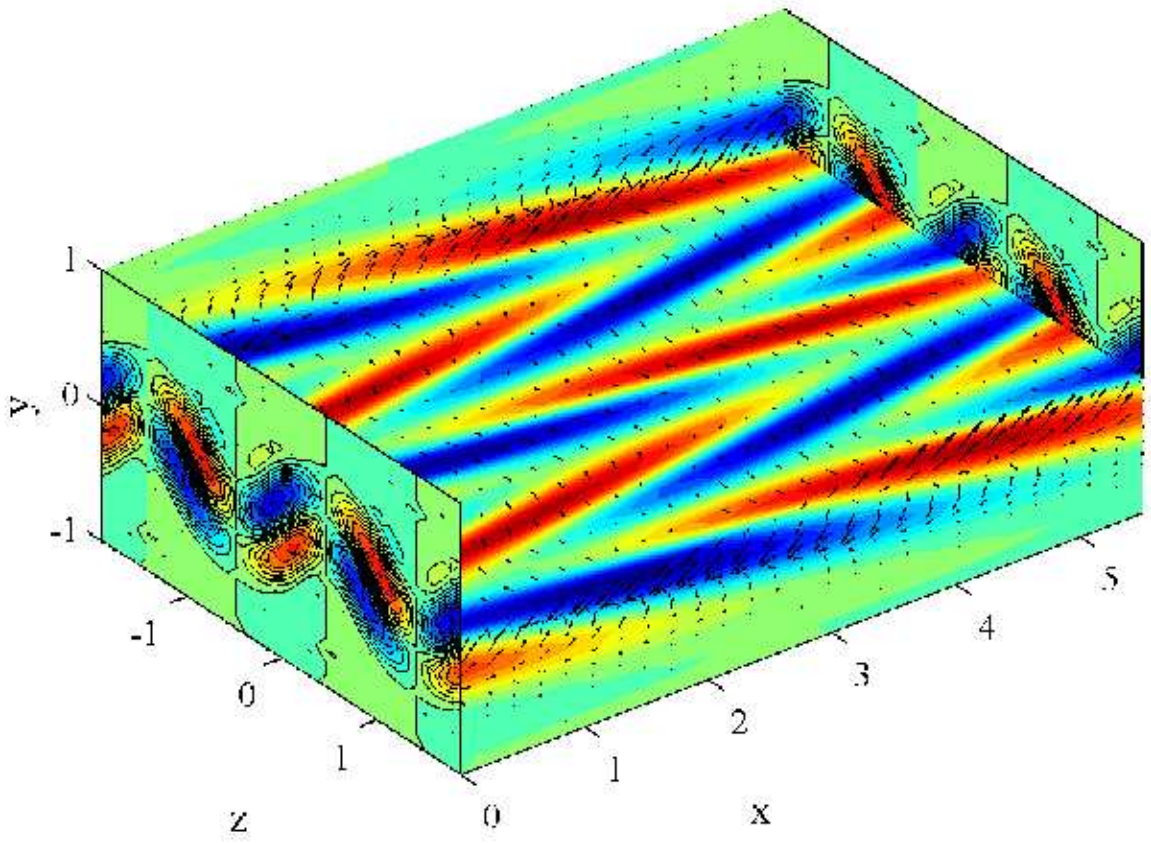

FIG. 17: (Color online) Velocity field of the adjoint in the energy inner product of the least stable mode with eigenvalue ($\sigma_r = -0.017$, $\sigma_i = 0$), for the equilibrium at STM excitation parameter $f = 8.4$. Velocity vectors are shown with contours of streamwise velocity. The adjoint is the optimal excitation of the mode. An initial condition consisting of the adjoint with unit energy excites the least stable mode a factor of 1900 greater than an initial condition consisting of the least stable mode itself with unit energy demonstrating that the mode amplitude derives almost entirely from non-normal growth processes. Parameters are as in Fig. 15.

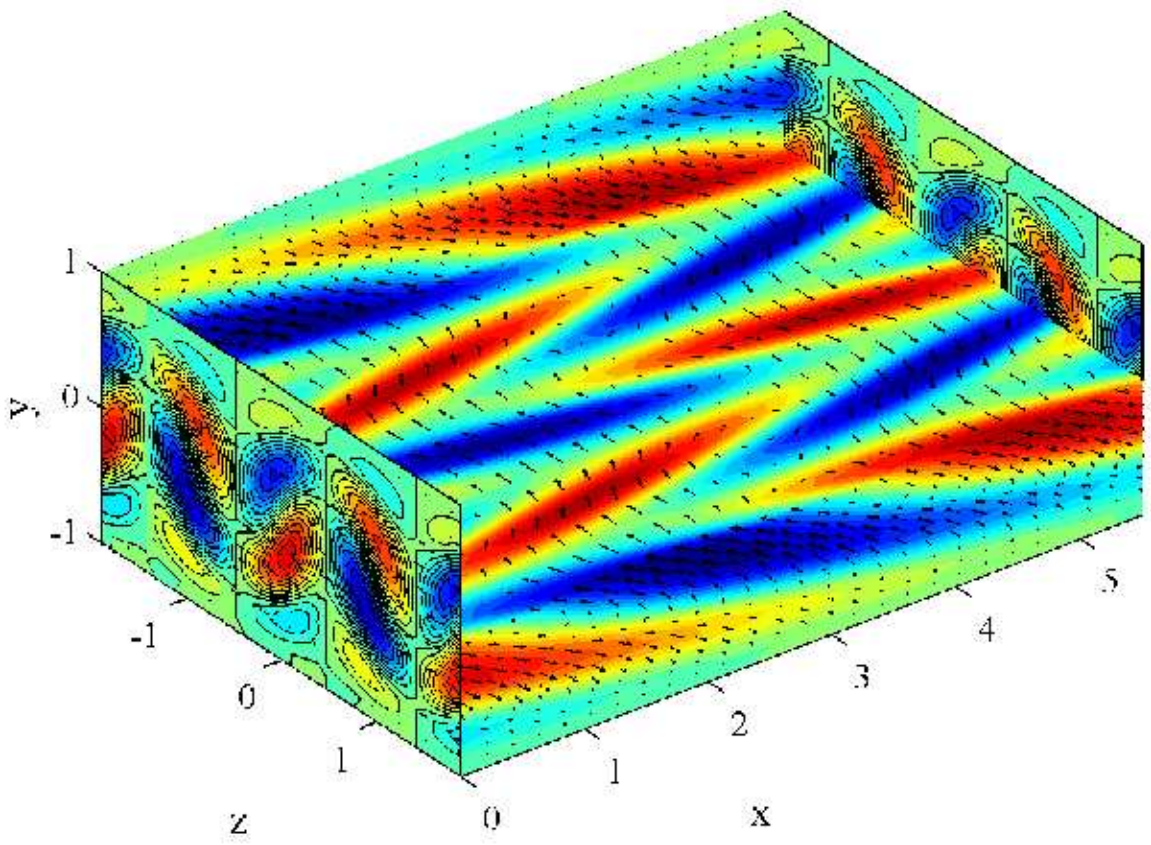

FIG. 18: (Color online) Velocity field at time $t = 0$ of the optimal perturbation that maximizes energy growth at $t = 10$ for the equilibrium flow with STM excitation parameter $f = 8.4$. Velocity vectors are shown with contours of streamwise velocity. Parameters are as in Fig. 15.

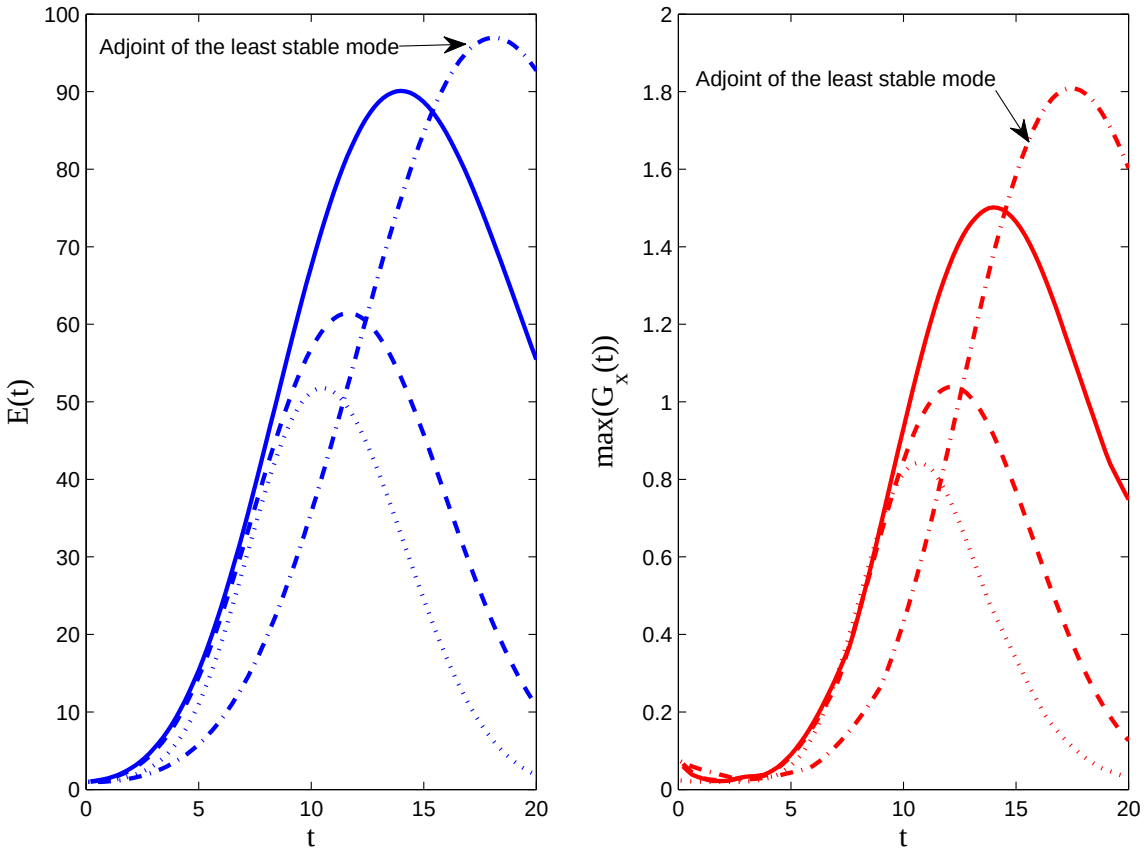

FIG. 19: (Color online) Left : Energy of the optimal perturbation that maximizes energy growth at $t = 10$ as a function of time for the equilibrium flow with STM excitation parameter $f = 8.4$ (solid), $f = 7.5$ (dashed) and for $f = 5$ for which there is no roll/streak; (dotted). Also shown is the energy growth associated with a unit energy initial condition consisting of the adjoint in the energy metric of the least damped mode for the equilibrium with $f = 8.4$ (dash-dot). Right: The time development of the maximum mean streamwise torque induced by the Reynold's stresses of the corresponding evolving optimals and the adjoint. This figure demonstrates that both the mode amplitude and its contribution to the streamwise mean torque are due to non-normal growth processes. All modes in these flows are exponentially stable (cf. Fig. 10a,c,d). Parameters are as in Fig. 15.

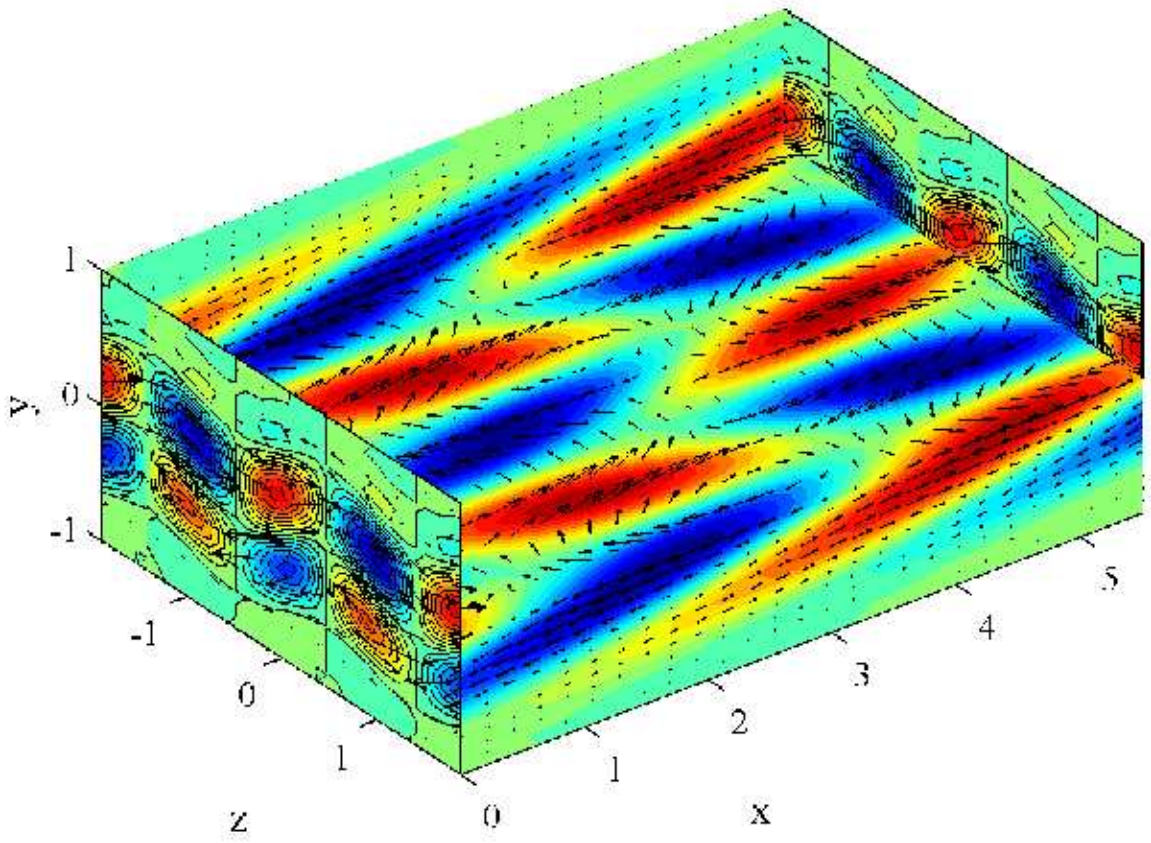

FIG. 20: (Color online) Velocity field at time $t = 15$ of the optimal perturbation that maximizes energy growth at $t = 10$ for the equilibrium flow with STM excitation parameter $f = 8.4$. Velocity vectors are shown with contours of streamwise velocity. Parameters are as in Fig. 15.

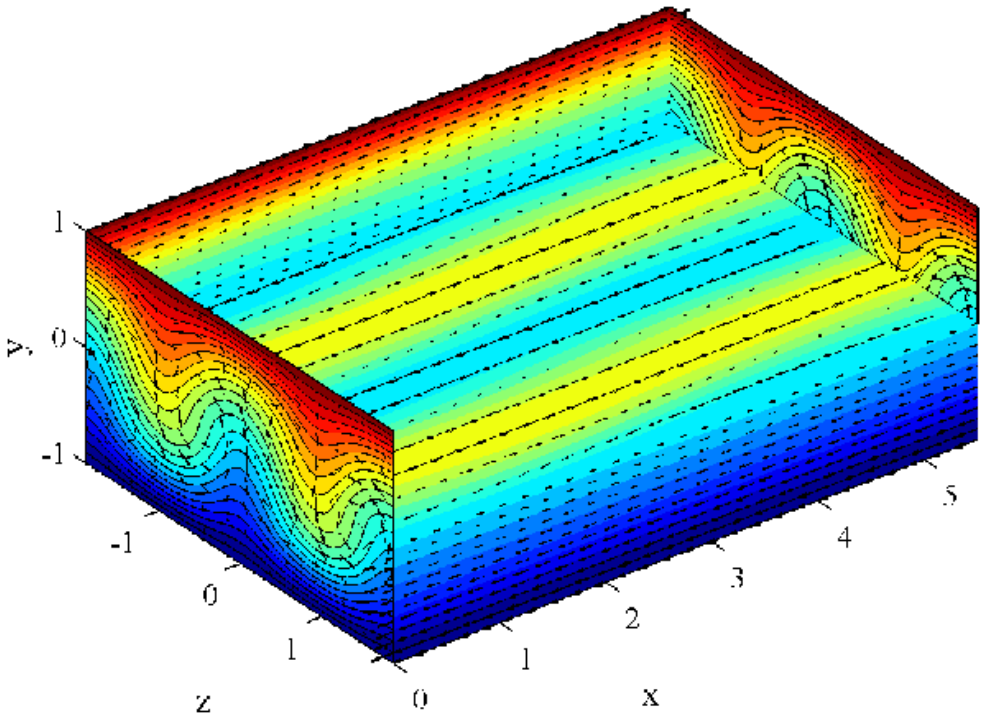

FIG. 21: (Color online) Velocity field (mean and perturbation) for the equilibrium flow with STM excitation parameter $f = 8.4$. Velocity vectors are shown with contours of streamwise velocity. The eddy field is a sum of the EOF's with amplitudes commensurate to their contribution to the total maintained eddy energy. The eddy field is dominated by the mean flow and the meandering of the streak in this laminar state is very slight. Parameters are as in Fig. 15.

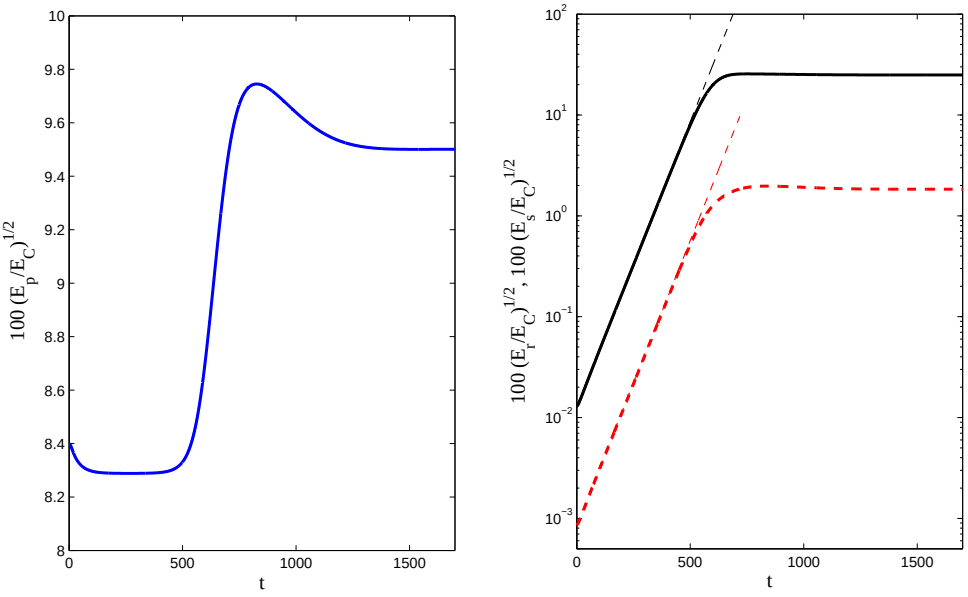

FIG. 22: (Color online) Left: Evolution of percent RMS eddy kinetic energy $100\sqrt{E_p/E_C}$ normalized by the RMS kinetic energy of the Couette flow after the structurally unstable spanwise independent equilibrium is perturbed by the most unstable streak perturbation shown in Fig. 8. The flow equilibrates to the roll/streak equilibrium shown in Fig. 9c and Fig. 13. Right: Evolution of the RMS streak energy $100\sqrt{E_s/E_C}$ and RMS roll energy $10^2\sqrt{E_r/E_C}$ is exponential with growth rate $\lambda = 0.014$. Parameters are as in Fig. 8, the STM excitation parameter is $f = 8.4$..

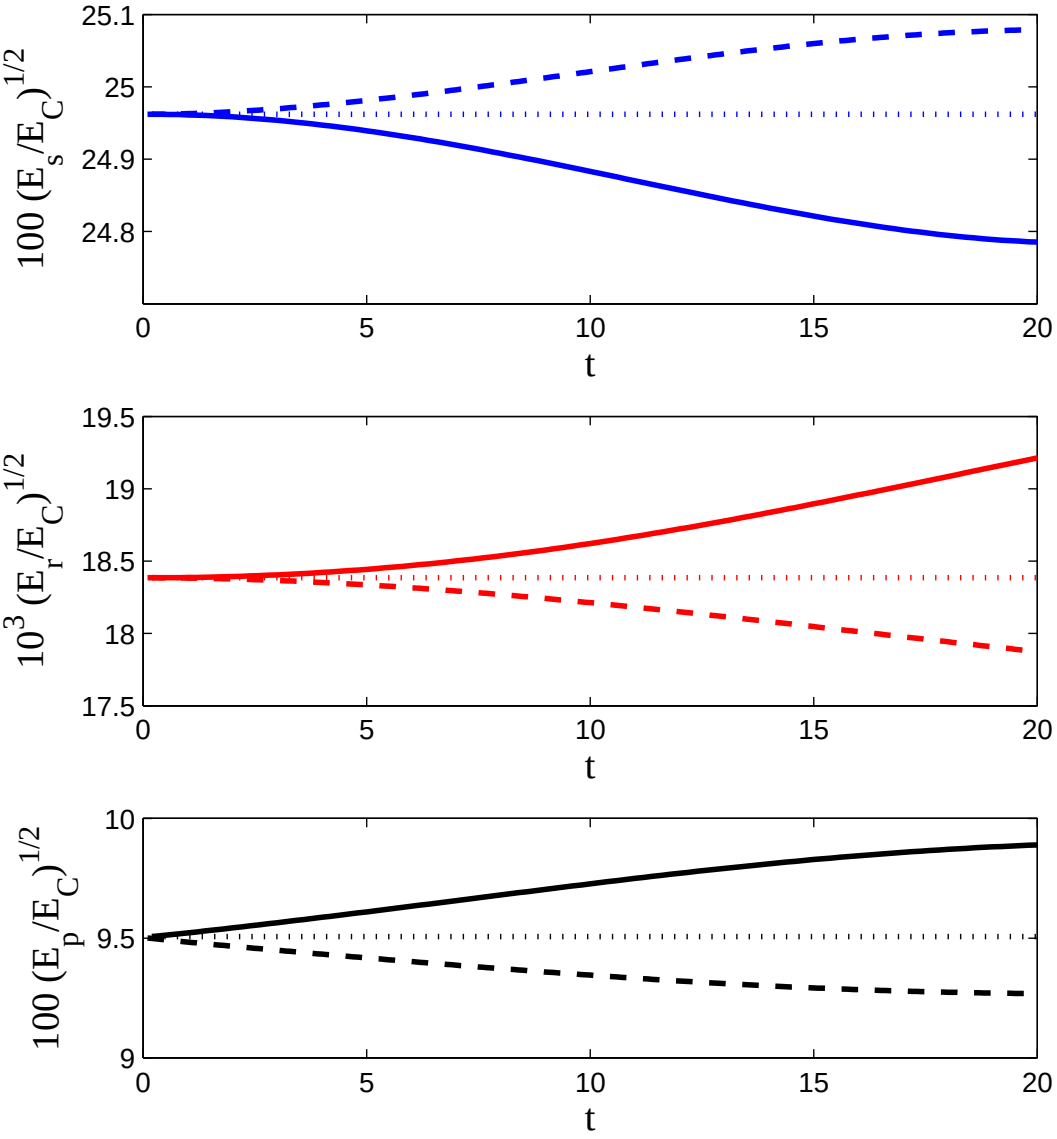

FIG. 23: (Color online) Percent RMS normalized streak amplitude $100\sqrt{E_s/E_C}$ (top panel), permil RMS normalized roll amplitude $10^3\sqrt{E_r/E_C}$ (middle panel), and percent RMS normalized perturbation velocity amplitude $100\sqrt{E_p/E_C}$ (bottom panel) as a function of time for decrease (solid) and increase (dashed) in the damping rate of the inflectional mode compared to its damping rate at equilibrium. The corresponding energies at equilibrium are also shown (dotted). The inflectional mode clearly damps rather than drives the streak. Parameters as in Fig. 15.

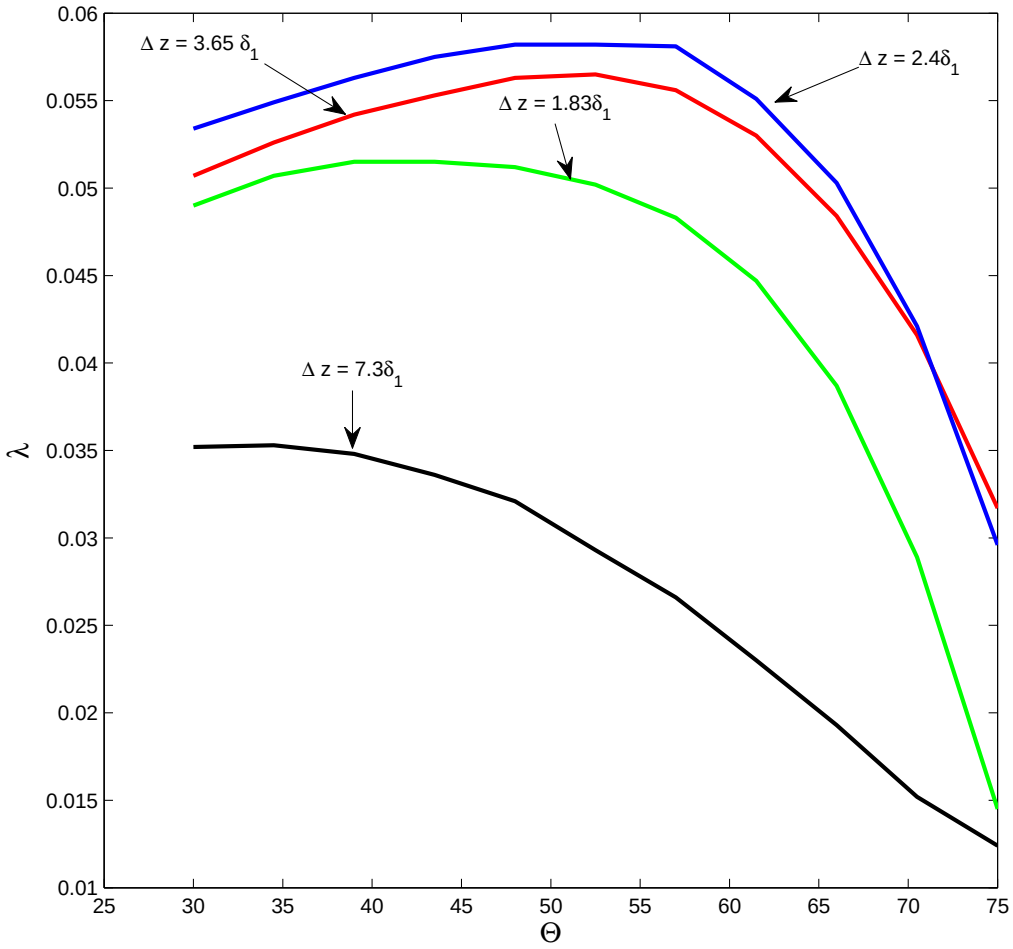

FIG. 24: (Color online) Growth rate, λ, of the structurally unstable streaks in a Blasius boundary layer as a function of perturbation structure obliqueness, $\Theta \equiv \tan^{-1}(m/k)$. The displacement thickness is $\delta_1 = 1.72$ and m is the wavenumber of the streak. Maximum growth rate occurs for $m = 3$ which corresponds to streak spacing $\Delta z = 2.4\delta_1$ or $50y^+$ wall units consistent with observations. Also shown are the growth rates for $m = 1, 2, 4$. The channel width is $L_z = 4\pi$, the Reynolds number is $R = 400$, the STM excitation parameter is $f = 10$ and the channel height is $L_y = 7$.